JHEP

Published for SISSA by Springer

Received: October 30, 2016
Revised: December 22, 2016
Accepted: December 22, 2016
Published: January 5, 2017

Top-quark loop corrections in Z+jet and $Z + 2$ jet production

John M. Campbell[a] **and R. Keith Ellis**[b]

[a] *Fermi National Accelerator Laboratory, PO Box 500, Batavia, IL 60510, U.S.A.*

[b] *Institute for Particle Physics Phenomenology, Department of Physics, Durham University, Durham DH1 3LE, U.K.*

E-mail: johnmc@fnal.gov, keith.ellis@durham.ac.uk

Abstract: The sophistication of current predictions for Z+jet production at hadron colliders necessitates a re-evaluation of any approximations inherent in the theoretical calculations. In this paper we address one such issue, the inclusion of mass effects in top-quark loops. We ameliorate an existing calculation of $Z + 1$ jet and $Z + 2$ jet production by presenting exact analytic formulae for amplitudes containing top-quark loops that enter at next-to-leading order in QCD. Although approximations based on an expansion in powers of $1/m_t^2$ can lead to poor high-energy behavior, an exact treatment of top-quark loops demonstrates that their effect is small and has limited phenomenological interest.

Keywords: NLO Computations, QCD Phenomenology

ArXiv ePrint: 1610.02189

doi:10.1007/JHEP01(2017)020

JHEP01(2017)020

Contents

JHEP01(2017)020

1 Introduction

The production of a Z-boson in association with jets is of considerable importance as a tool for understanding the Standard Model (SM). The Z+jet process has been proposed as a probe of both parton distribution functions and the high-energy running of the strong coupling, α_s. The production of more than one jet is especially important in the environment of the LHC, where typical jet reconstruction algorithms routinely result in multiple jets. This means that Z+jets processes represent significant backgrounds in many searches for New Physics, notably when the Z-boson decays to neutrinos so that it is a source of large missing transverse energy. Therefore they must be predicted precisely within the SM.

In order to obtain the level of theoretical precision required to match the small experimental uncertainties [1, 2], it is imperative to perform perturbative calculations of Z+jet processes beyond the leading order. The dominant source of corrections arises from QCD, with next-to-leading order (NLO) calculations available for processes involving up to four jets [3–7]. The expected experimental precision of measurements of the $Z + 1$ jet state has motivated the calculation of this process to the next order (NNLO) [8–11], so that experimental and theoretical uncertainties in this case are commensurate over a relatively large kinematic range. At this level of theoretical accuracy it is also necessary to have control over corrections arising from the electroweak sector. These effects are known for up to two jets in the final state [12–14].

With these results in hand it is important to revisit assumptions and approximations inherent in some of the calculations performed so far. One such approximation relates to the inclusion of the effect of the top quark in one-loop virtual corrections to these processes. Since the mass of the top quark introduces a new scale into the problem, including its effect results in a significantly more complex analytic calculation than the usual case in which all quarks are considered massless. In their classic 1997 paper [15], Bern, Dixon and Kosower (BDK) gave results for such contributions to the $Z+1$ and $Z+2$ jet processes by performing a large mass expansion in the top-quark mass. Although this approximation was appropriate in the last century, and in particular for e^+e^- annihilation at LEP energies, it may no longer be appropriate at the LHC and higher energy machines where scales above the top quark mass are probed.

In this paper we shall compute a class of one-loop corrections to $Z + 1$ and $Z + 2$ jet processes, specifically considering the effects of fermion loops in which the full dependence on the top-quark mass is retained. The one-loop results for these processes can be obtained with a number of numerical programs, such as MadLoop/Madgraph_aMC@NLO [16, 17], GoSam [18, 19] and OpenLoops [20], since the presence of a massive particle does not complicate the computation in the same way. Although the results of these programs are therefore sufficient for many practical purposes, the existence of analytic results enables a more efficient and numerically-stable evaluation of the one-loop amplitudes. This has been important for their use in other applications, such as the evaluation of NNLO corrections to Z+jet production [9] and matching jet substructure observables at next-to-next-to-leading logarithmic accuracy [21].

JHEP01(2017)020

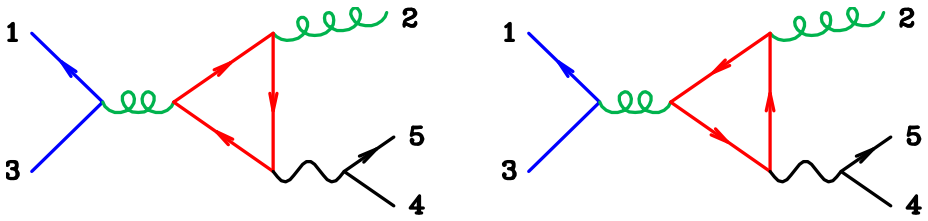

Figure 1. Examples of fermion loop diagrams contributing to $Z + 1$ jet production. The only non-zero contribution enters through the axial coupling of the Z-boson to third-generation quarks.

The amplitudes that we have computed may be useful for other crossed, or related, processes and are provided in the appendix. The phenomenological impact of these calculations is assessed for the $Z+1$ jet case in section 2 and for the $Z+2$ jet process in section 3.

2 Top-loop effects in $Z + 1$ jet production

In the case of $Z + 1$ jet production, top-quark loop contributions only enter through diagrams such as the ones shown in figure 1. Furry's theorem means that diagrams containing a vector coupling of the Z-boson to the quark loop vanish, so that only the axial coupling contributes. In fact, since we consider all quarks other than the top quark to be massless, due to the opposite weak isospin of up- and down-type quarks, the only contribution from these diagrams comes from the third generation. In the original BDK treatment of these diagrams [15], these contributions are computed in the limit that $m_t \to \infty$, with the leading term in a $1/m_t^2$ expansion retained. We have recomputed these contributions retaining the full top-quark mass dependence; the analytic form of the amplitudes representing this contribution is given in appendix A.

This expansion can be extended to include higher-order terms but in the high-energy regime this can lead to problems since the expansion is properly of the form s/m_t^2, where s becomes large. This is illustrated in figure 2 (left), which shows results obtained using the `CT14.NN` pdf set [22] with both renormalization and factorization scales equal to $H_T/2$, where H_T is the scalar sum of the transverse momenta of all leptons and partons. The leading term in the expansion (as presented in BDK) agrees very well with the exact result over the range shown. Including further terms in the $1/m_t^2$ expansion spoils this agreement. Although the exact treatment and the $1/m_t^6$ approximation agree up to jet transverse momenta around 1 TeV, beyond that the approximation is no longer under control and results in a wildly different prediction for the spectrum. The lower panel shows the ratio of the approximation with the leading term to the exact result. The two differ by around 0.7% for a jet with 3 TeV transverse momentum. Since the number of events in this region is negligible this is not a significant difference. We conclude that, although the exact result should be preferred, there is no observable impact on the phenomenology of this process when using only the leading term in the $1/m_t^2$ expansion.

At a 100 TeV collider the differences are more significant, as shown in figure 2 (right). Even for 10 TeV jets, which would be abundant at such a collider, the effect of the approximate top-quark loop is a few percent. Since this is at the same level as the NNLO corrections, it is important that the exact result be available and taken into account.

JHEP01(2017)020

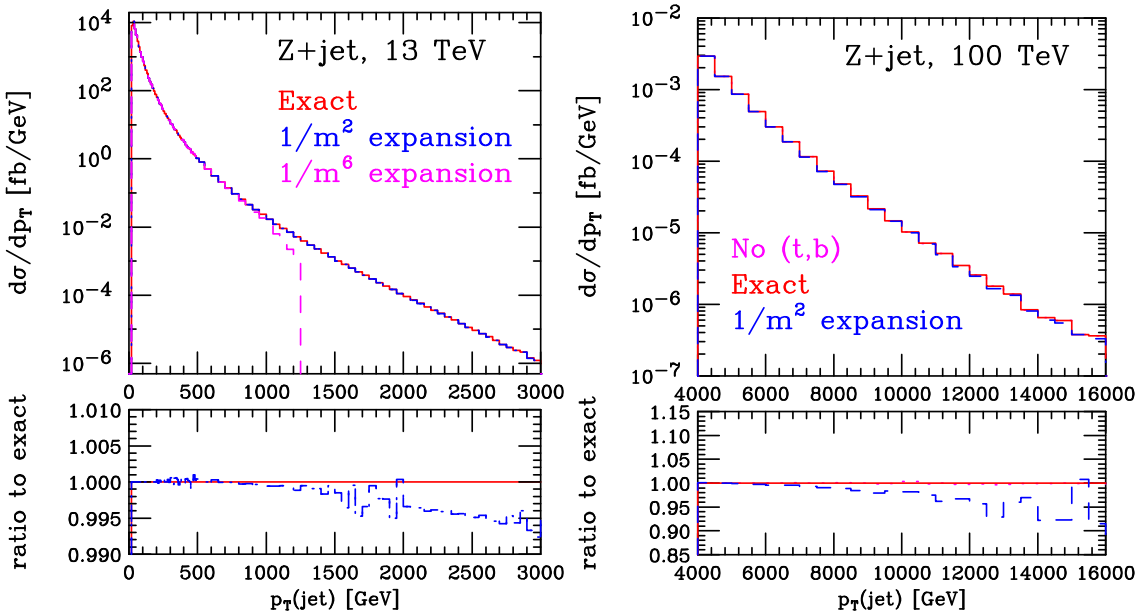

Figure 2. The jet p_T spectrum for Z+jet production at NLO, computed for the 13 TeV LHC (left) and a 100 TeV pp collider (right). The calculation uses a scale $\mu_r = \mu_f = H_T/2$ and no cuts are applied apart from $p_T(\text{jet}) > 25\,\text{GeV}$. The red (solid) histogram corresponds to the exact result while the blue (dot-dash) and magenta (dash) histograms represent the large-mass expansion up to $1/m_t^2$ and $1/m_t^6$ respectively, as detailed in the text.

Since the thrust of this paper is to examine the impact of the top quark loops themselves, not to perform an exhaustive analysis of the Z+jet process, we have not considered the uncertainty associated with the choice of scales used in figure 2. Indeed, the effects discussed here may be much smaller than other extant theoretical shortcomings. The residual scale dependence in NNLO calculations of the $Z + 1$ jet process [8–11] is typically at the level of a few percent in the bulk, but much larger at high jet transverse momentum. The effect of virtual electroweak corrections is also known to be significant in this region [12–14] and approximations for combining the effect of QCD and electroweak corrections gives rise to a further uncertainty.

3 Top-loop effects in $Z + 2$ jet production

The $Z + 2$ jet process is sensitive to a much wider range of virtual corrections that involve a closed loop of top quarks. This is partly due to the fact that the process is represented by two separate parton-level reactions (and all appropriate crossings):

$$0 \to q(-p_1) + \bar{q}(-p_2) + g(p_3) + g(p_4) + e^+(p_5) + e^-(p_6)\,, \tag{3.1}$$

$$0 \to q(-p_1) + \bar{Q}(-p_2) + Q(p_3) + \bar{q}(p_4) + e^+(p_5) + e^-(p_6)\,. \tag{3.2}$$

The labels q and Q refer to two (possibly distinct) flavours of massless quark. We will refer to these by the abbreviated forms, $q\bar{q}ggZ$ and $q\bar{q}Q\bar{Q}Z$ processes. In the original BDK paper, all of the top-quark loop contributions have been included using the $1/m_t^2$ expansion.

JHEP01(2017)020

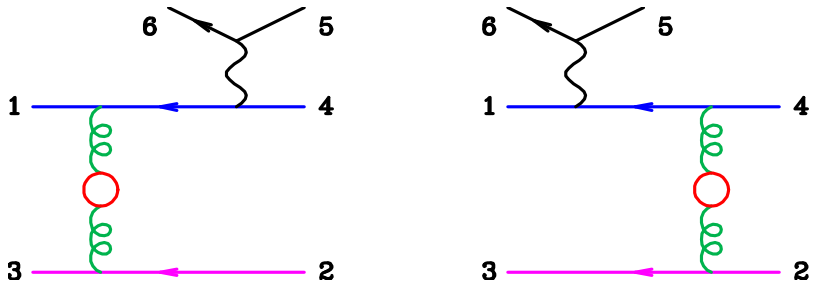

Figure 3. Vacuum polarization diagrams contributing to the $q\bar{q}Q\bar{Q}Z$ process, where the Z-boson couples to an external line of light quarks.

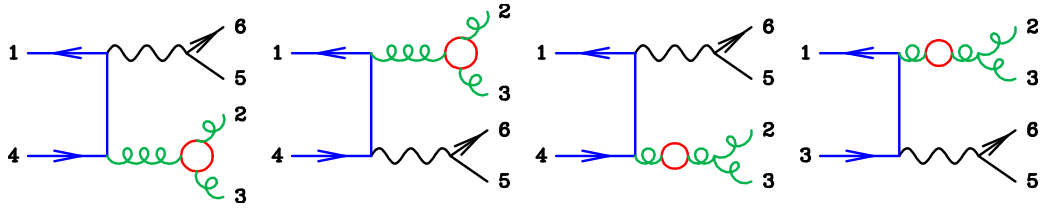

Figure 4. Examples of fermion loop (top quark) diagrams in which the Z-boson couples to an external line of light quarks in the $q\bar{q}ggZ$ process.

In this work we have computed all of the corrections retaining the full dependence on the top-quark mass. The addition of the mass complicates the analytic form of the amplitudes but we have still obtained relatively compact expressions. This is achieved through the use of analytic unitarity methods for computing one-loop box and triangle coefficients [23–25] and by recycling BDK results for the massless case whenever possible. Full details of our calculation, including explicit expressions for all amplitudes, are presented in appendices B and C.

The top-quark loop contributions can be categorized according to the manner in which the Z-boson couples to the partons:

1. Contributions where the Z boson couples to the light quark line. These correspond to vacuum polarization contributions to the $q\bar{q}Q\bar{Q}Z$ process shown in figure 3 and to the loop corrections to the $q\bar{q}ggZ$ process depicted in figure 4. These amplitudes are described in detail in appendices B.3 and C.3.

2. A vector coupling of the Z-boson to a closed loop of top quarks, occurring in diagrams such as the one shown in figure 5(c). These are only present in the $q\bar{q}ggZ$ process and are described in appendix C.4.

3. An axial coupling of the Z-boson to a closed loop of quarks, as shown in figures 5 and 6 for the $q\bar{q}ggZ$ and $q\bar{q}Q\bar{Q}Z$ processes, respectively. This contribution vanishes for all but the third generation of quarks, whose effect is captured here. For the $q\bar{q}Q\bar{Q}Z$ process these corrections are discussed in appendix B.4 while the corresponding contributions to the $q\bar{q}ggZ$ process are detailed in appendices C.5 and C.6.

JHEP01(2017)020

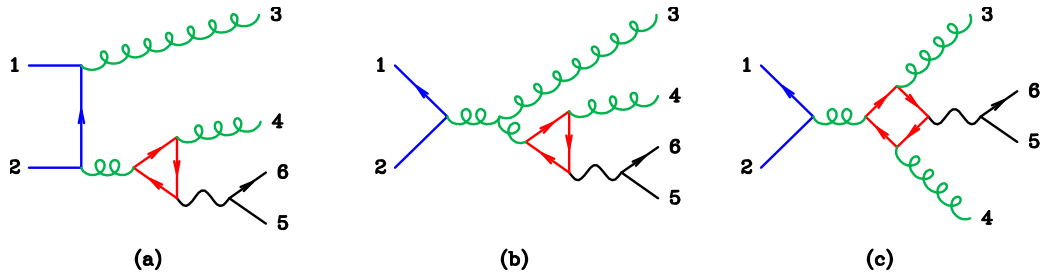

Figure 5. Examples of fermion loop diagrams contributing when the Z couples to a heavy quark line through either a vector or an axial coupling. With a vector coupling the triangle diagrams vanish, and hence only the box diagrams contribute.

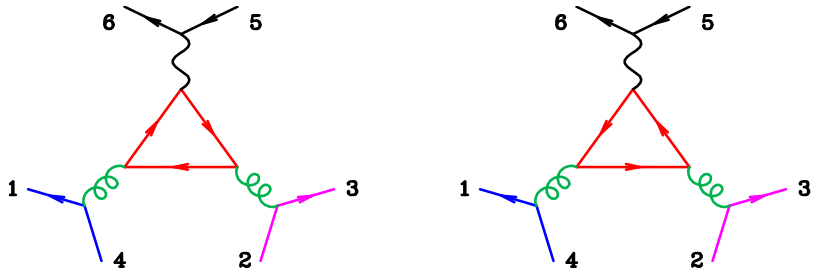

Figure 6. Quark loop diagrams involving the axial coupling of the Z-boson in the $q\bar{q}Q\bar{Q}Z$ process.

We will now examine the effect of each of these contributions separately, both in the $1/m_t^2$ approximation used in the BDK form of the amplitudes and with the improved treatment provided by the exact expressions presented here. Our calculation is performed by incorporating our newly-calculated amplitudes in the Monte Carlo program MCFM [26–28], which already includes a complete calculation of $Z + 2$ jet production at NLO that makes use of the BDK loop amplitudes. The expressions for the amplitudes with the exact top-mass dependence are written in terms of the scalar integrals described in appendix D, that are evaluated numerically using the `ff` [29, 30] and `QCDLoop` [31, 32] libraries.

For all of the results in this section we will consider the production of an on-shell Z-boson that decays to an electron-positron pair, with no cuts applied to the leptons. This is a choice made for the presentation of our results, and not an intrinsic limitation of MCFM. We use the same pdf set and scale choices as in section 2.

3.1 Results: 100 TeV collider

Since we expect the problems associated with the $1/m_t^2$ expansion used in the original BDK expressions to be exacerbated at high energies, we first present results for a putative 100 TeV proton-proton collider. We define jets using the anti-k_T clustering algorithm with a jet separation $R = 0.5$ and demand that they satisfy,

$$p_T(\text{jet}) > 500 \text{ GeV}\,, \qquad y(\text{jet}) < 4\,. \tag{3.3}$$

A comparison of the NLO predictions for the lead jet transverse momentum, with various levels of sophistication, is shown in figure 7. The approximation of the contributions with the Z-boson coupled to a top-quark loop through axial and vector couplings lead to

JHEP01(2017)020

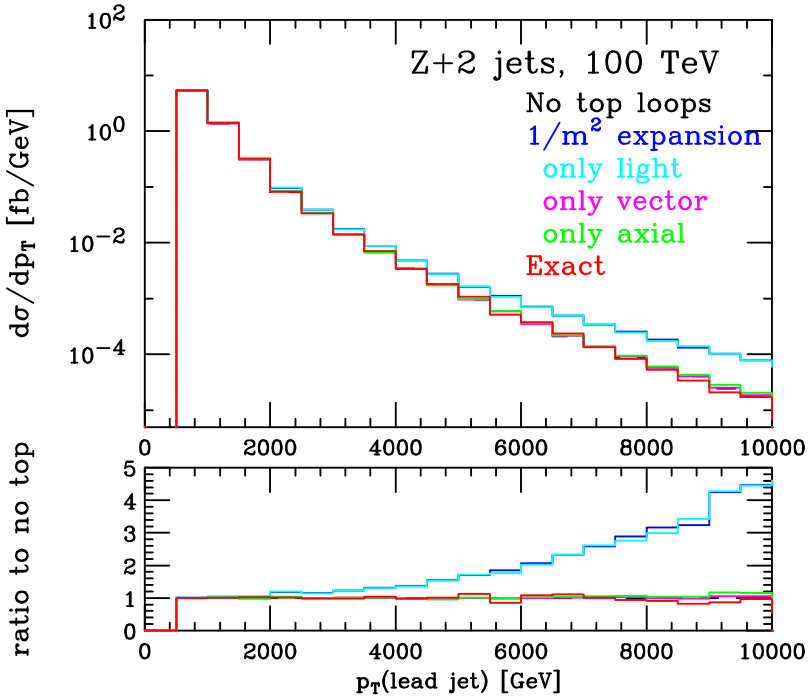

Figure 7. Upper panel: the distribution of the transverse momentum of the leading jet in $Z+2$ jet events at 100 TeV. Predictions are shown with no top-quark loops included, using the $1/m_t^2$ approximation and with the exact result (including all contributions). The exact, only vector and only axial histograms are almost indistinguishable from the result with no top-quark loops. Lower panel: the ratio of the predictions of the approximate treatment to the one in which no top-quark loops are included.

relatively small deviations in this range. In contrast, approximating the contributions that involve the Z-boson coupling to light quarks in the same way leads to substantial errors at jet transverse momenta of about 3 TeV and higher. The NLO rate is over-estimated by a factor of four for a 10 TeV jet. Using the exact result for the top-quark loops yields a prediction that is essentially unchanged from the one in which they are not included at all.

3.2 Results: LHC at $\sqrt{s} = 14$ TeV

We now turn to results of more immediate interest, namely predictions for the LHC operating at $\sqrt{s} = 14$ TeV. We adjust the jet cuts accordingly and now demand,

$$p_T(\text{jet}) > 50 \text{ GeV}\,, \qquad y(\text{jet}) < 2.5\,. \tag{3.4}$$

A comparison of our calculations under these cuts is shown in figure 8. Note that, in comparison to the previous figure, the lower panel has a much smaller scale since we consider transverse momenta for the jet that are much lower. In addition, having observed that the effect of the diagrams in which the Z-boson couples to a top-quark loop is small, in this case we simply show the sum of the contributions from the vector and axial couplings of the Z-boson to top quarks. As expected, at the energies that are accessible at the LHC

JHEP01(2017)020

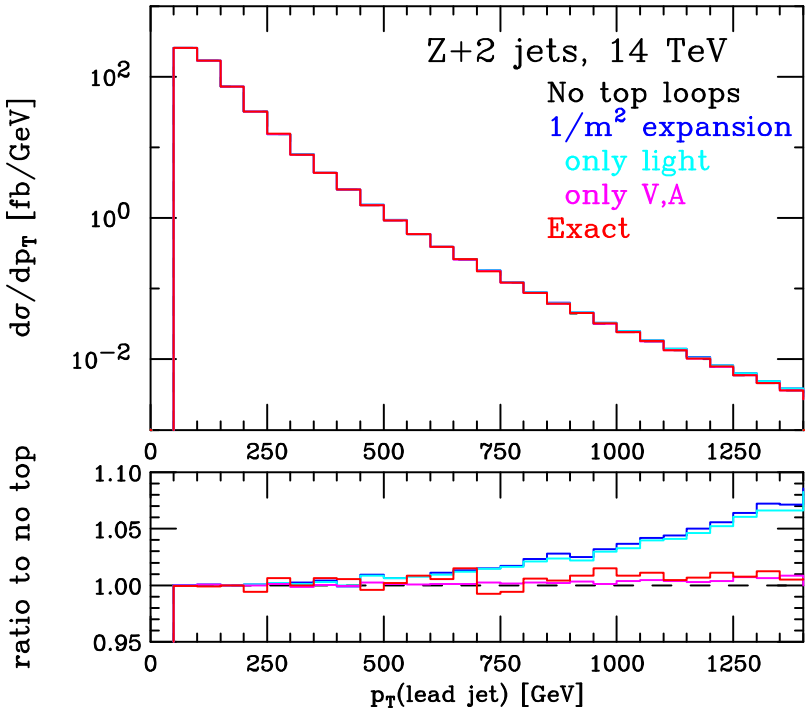

Figure 8. Upper panel: the distribution of the transverse momentum of the leading jet in $Z+2$ jet events at 14 TeV. Predictions are shown with no top-quark loops included, using the $1/m_t^2$ approximation and with the exact result (including all contributions). The exact, and only vector and axial, histograms are barely distinguishable from the result with no top-quark loops. Lower panel: the ratio of the predictions of the approximate treatment to the one in which no top-quark loops are included.

the error made when using the $1/m_t^2$ approximation is much less severe. Even at a jet transverse momentum of 1 TeV it only results in a 4% deviation from the result with no top-loops included. The effect of the approximation on the cross-section for both jets above 50 GeV is an enhancement of a mere 0.05%.

4 Conclusions

In this paper we have reviewed the importance of top-quark loops in NLO corrections to $Z+1$ jet and $Z+2$ jet production. To do so, we have computed the effect of these loops with an exact treatment of the top-quark mass and given analytic forms for all the relevant amplitudes. We find that the effect of these loops is very small and not important for phenomenology at the LHC. For a putative 100 TeV proton-proton collider the effects are more significant and, for the $Z+1$ jet case, lead to a few percent change in the prediction for jets with transverse momentum of 10 TeV. Attempting to include the effect of these loops by using an expansion in powers of $1/m_t^2$ leads to the theoretical prediction being over-estimated due to poor high-energy behaviour. While this may be at a level that is tolerable at the LHC, it can lead to results at 100 TeV that are incorrect by factors of two or more.

JHEP01(2017)020

Boson	Feynman rule	Coupling
γ	$-ieQ^f\gamma^\mu$	
Z	$-ie\gamma^\mu(v_V^f - v_A^f\gamma_5)$	$v_V^f = \frac{(\tau_3^f - 2Q^f \sin^2\theta_W)}{\sin 2\theta_W}$, $v_A^f = \frac{\tau_3^f}{\sin 2\theta_W}$, $\tau_3^f = \pm\frac{1}{2}$
	$-ie\gamma^\mu(v_L^f\gamma_L + v_R^f\gamma_R)$	$v_L^f = \frac{(2\tau_3^f - 2Q^f \sin^2\theta_W)}{\sin 2\theta_W}$, $v_R^f = \frac{-2Q^f \sin^2\theta_W}{\sin 2\theta_W}$

Table 1. Feynman rules and couplings of a photon and a Z to a fermion-antifermion pair. For massless fermions it is convenient to use the left- and right-handed couplings, rather than the vector and axial couplings, so both are shown. Q^f is the charge of the fermion in units of the positron electric charge.

Acknowledgments

RKE would like to thank the Fermilab theory group for hospitality during the preparation of this paper. The research of JMC is supported by the US DOE under contract DE-AC02-07CH11359.

A Five point amplitude $A(1_q, 2_g, 3_{\bar{q}}, 4_{\bar{e}}, 5_e)$

In this appendix we consider the five-point amplitudes that enter the calculation of $Z+1$ jet production. Specifically, we consider the process:

$$0 \to q(-p_1) + g(p_2) + \bar{q}(-p_3) + e^+(p_4) + e^-(p_5)\,. \tag{A.1}$$

A.1 Tree graphs

We write the tree-level amplitude as,

$$\mathcal{A}_5^{\rm tree} = 2e^2 g\big(-Q^q + v_{L,R}^e v_{L,R}^q \mathcal{P}_Z(s_{45})\big)\,\big(T^{a_2}\big)_{i_1}^{\bar{\imath}_3}\, A_5^{\rm tree}(1_q, 2_g, 3_{\bar{q}})\,, \tag{A.2}$$

where we have omitted the labels of the electron-positron pair, (5 and 4 respectively). We further define

$$s_{ij} = (p_i + p_j)^2, \quad s_{ijk} = (p_i + p_j + p_k)^2\,. \tag{A.3}$$

e is the QED coupling, g the QCD coupling, Q^q is the charge of quark q in units of e, (the positron charge), and the ratio of Z and photon propagators is given by

$$\mathcal{P}_Z(s) = \frac{s}{s - M_Z^2 + i\,\Gamma_Z\,M_Z}\,, \tag{A.4}$$

where M_Z and Γ_Z are the mass and width of the Z. The definition of the Z/γ^* couplings is given in table 1. Colour matrices are normalized such that

$$\mathrm{Tr}\,T^{a_1}T^{a_2} = \delta^{a_1\,a_2}\,. \tag{A.5}$$

For the tree amplitude $A_5(1_q^+, 2_g^+, 3_{\bar{q}}^-, 4_{\bar{e}}^-, 5_e^+)$, the result is,

$$A_5^{\rm tree}(1_q^+, 2_g^+, 3_{\bar{q}}^-) = -i\frac{\langle 3\,4\rangle^2}{\langle 1\,2\rangle\langle 2\,3\rangle\langle 4\,5\rangle}\,. \tag{A.6}$$

We note that this matrix element has the same sign as BDK, eq. (D1), as do all of the results in this section. The $\langle i\,j\rangle$ and $[i\,j]$ are the normal spinor products for massless vectors, such that $\langle i\,j\rangle[j\,i] = s_{ij}$. For details of their definition see refs. [33, 34].

A.2 Fermion loop corrections to the tree level amplitude

The one-loop colour decomposition is given by

$$\begin{aligned}\mathcal{A}_5^{1-\text{loop}}(1_q,2_g,3_{\bar{q}}) = 2e^2\,g^3\Big\{&\left(-Q^q + v^e_{L,R}v^q_{L,R}\,\mathcal{P}_Z(s_{45})\right)\\ &\times(T^{a_2})_{i_1}{}^{\bar{\imath}_3}\left[N_c A_{5;1}(1_q,2_g,3_{\bar{q}}) + \frac{1}{N_c}A_{5;2}(1_q,3_{\bar{q}};2_g)\right]\\ &+2\sum_{f=t,b} v^f_A\,v^e_{L,R}\,\mathcal{P}_Z(s_{45})(T^{a_2})_{i_1}{}^{\bar{\imath}_3}\,A^f_{5;3}(1_q,3_{\bar{q}};2_g)\Big\}\,. \end{aligned} \tag{A.7}$$

The results for the functions $A_{5;1}$ and $A_{5;2}$ are given in BDK [15]. Since they do not involve fermion loops we do not repeat them here. The function $A_{5;3}$ contains the terms where a Z couples to a loop of quarks via the axial coupling, as shown in figure 1, where our conventions for the overall coupling factors are given in table 1. If we consider all quarks except the top to be massless then there is a net contribution only for the third generation, because of the opposite weak isospin of the up- and down-type quarks.

The result for the leading order interfered with the NLO and summed over colours is given in terms of partial amplitudes as,

$$\begin{aligned}\sum_{\text{colors}}[\mathcal{A}_5^*\mathcal{A}_5]_{\text{NLO}} = 8e^4\,g^4\,(N_c^2-1)\,N_c\,\text{Re}\Big\{&\left(-Q^q + v^e_{L,R}v^q_{L,R}\,\mathcal{P}^*_Z(s_{45})\right)A_5^{\text{tree}*}(1_q,2_g,3_{\bar{q}})\\ &\times\left[\left(-Q^q + v^e_{L,R}v^q_{L,R}\,\mathcal{P}_Z(s_{45})\right)\left[A_{5;1}(1_q,2_g,3_{\bar{q}}) + \frac{1}{N_c^2}A_{5;2}(1_q,3_{\bar{q}};2_g)\right]\right.\\ &\left.+\frac{2}{N_c}\sum_{f=t,b} v^f_A\,v^e_{L,R}\,\mathcal{P}_Z(s_{45})A^f_{5;3}(1_q,3_{\bar{q}};2_g)\right]\Big\}\,. \end{aligned} \tag{A.8}$$

Note that the axial part $A^f_{5;3}$ depends on the flavour of the quark (f) and we have to sum over the contributions of the top and bottom loops. We choose to follow the conventions of the original BDK presentation and write the subleading contributions with permuted momentum labels. In this scheme we further define

$$A^f_{5;3}(1_q,2_{\bar{q}};3_g) = ic_\Gamma A^f_{\text{ax}}(1^+_q,2^-_{\bar{q}};3^+_g)\,, \tag{A.9}$$

with

$$c_\Gamma = \frac{1}{(4\pi)^{2-\epsilon}}\frac{\Gamma(1+\epsilon)\Gamma^2(1-\epsilon)}{\Gamma(1-2\epsilon)}\,. \tag{A.10}$$

In this case the terms of order ϵ and higher in c_Γ are not needed because the amplitude is finite. The result for this amplitude is, including both the top and bottom contributions,

$$A^{t,b}_{\text{ax}}(1^+_q,2^-_{\bar{q}};3^+_g) = 2\frac{[5\,3][3\,1]\langle 2\,4\rangle}{s_{45}}\Big[f(m_t;0,s_{12},s_{45}) - f(m_b;0,s_{12},s_{45})\Big]\,, \tag{A.11}$$

where m_f is the mass of the quark running in the triangular loop. We shall take the bottom quark to be massless, $m_b = 0$.

JHEP01(2017)020

The function f is the axial triangle function that depends on m_f, for which results have been given in ref. [15] and are detailed in appendix F. For a massive quark, such as the top quark, in the special case where one of the legs of the triangle is light-like, we have, (cf. eq. (F.13))

$$f(m;0,q_1^2,q_3^2) = \frac{1}{2(q_3^2-q_1^2)}\Bigg[1 + 2m^2 C_0(q_1,q_3;m,m,m) + \left(\frac{q_3^2}{(q_3^2-q_1^2)}\right)\Big[B_0(q_3;m,m) - B_0(q_1;m,m)\Big]\Bigg]. \tag{A.12}$$

B_0 and C_0 are the scalar integral functions defined in appendix D. In the limit $m \to \infty$ we get

$$f(m;0,q_1^2,q_3^2) = \frac{1}{24m^2}\left[1 + \frac{(2q_1^2+q_3^2)}{15m^2} + \frac{(2q_1^2q_3^2+3q_1^4+q_3^4)}{140m^4}\right] + O(1/m^8)\,. \tag{A.13}$$

The result for a massless quark is,

$$f(0;0,q_1^2,q_3^2) = \frac{1}{2(q_3^2-q_1^2)}\left[1 + \frac{q_3^2}{(q_3^2-q_1^2)}\log\left(\frac{q_1^2}{q_3^2}\right)\right] = \frac{1}{2q_3^2}L_1\left(\frac{q_1^2}{q_3^2}\right), \tag{A.14}$$

where L_0, L_1 are the cut-completed functions,

$$L_0(r) = \frac{\ln(r)}{1-r}, \quad L_1(r) = \frac{L_0(r)+1}{1-r}\,. \tag{A.15}$$

Summing over the third generation isodoublet in the limit $m_b = 0$ we get,

$$A_{\rm ax}^{t,b}(1_q^+, 2_{\bar q}^-; 3_g^+) = \frac{[5\,3][3\,1]\langle 2\,4\rangle}{s_{45}}\left[2\,f(m_t;0,s_{12},s_{45}) - \frac{1}{s_{45}}L_1\left(\frac{-s_{12}}{-s_{45}}\right)\right]. \tag{A.16}$$

Keeping only the leading term in the $m \to \infty$ limit given in eq. (A.13), this agrees with BDK, eq. (D.11).

B Six point amplitude, $A(1_q, 2_{\bar Q}, 3_Q, 4_{\bar q}, 5_{\bar e}, 6_e)$

We now consider processes with one more parton in the final state, starting with processes containing four quarks.[1]

B.1 Tree graphs

The general decomposition for the tree process requires that we include the two terms corresponding to the Z/γ^* attaching to one or the other of the quark lines,

$$\begin{aligned}\mathcal{A}_6^{\rm tree}(1_q,2_{\bar Q},3_Q,4_{\bar q}) = 2e^2g^2\Bigg[&\Big(-Q^q + v_{L,R}^e v_{L,R}^q\,\mathcal{P}_Z(s_{56})\Big)A_6^{\rm tree}(1_q,2_{\bar Q},3_Q,4_{\bar q}) \\ &+\Big(-Q^Q + v_{L,R}^e v_{L,R}^Q\,\mathcal{P}_Z(s_{56})\Big)A_6^{\rm tree}(3_Q,4_{\bar q},1_q,2_{\bar Q})\Bigg] \\ &\times\left(\delta_{i_1}^{\bar i_2}\delta_{i_3}^{\bar i_4} - \frac{1}{N_c}\delta_{i_1}^{\bar i_4}\delta_{i_3}^{\bar i_2}\right).\end{aligned} \tag{B.1}$$

[1] We find that the overall sign for the six point processes, using the Feynman rules of ref. [35], is opposite to that of BDK. Since it is an overall sign it is of no importance; to allow our results to be used as a supplement to BDK, we have adjusted our overall sign to agree with the conventions of BDK.

JHEP01(2017)020

The result for the tree process is,

$$A_6^{\rm tree}(1_q^+,2_{\bar{Q}}^+,3_Q^-,4_{\bar{q}}^+,5_{\bar{e}}^-,6_e^+) = -i\left[\frac{[1\,2]\langle 4\,5\rangle\langle 3|(1+2)|6]}{s_{23}s_{56}s_{123}} + \frac{\langle 3\,4\rangle[1\,6]\langle 5|(3+4)|2]}{s_{23}s_{56}s_{234}}\right]. \quad \text{(B.2)}$$

This result is in agreement with BDK eq. (12.3).

B.2 One-loop results general structure

The general structure of the decomposition at one loop is [36]

$$\begin{aligned}
&\mathcal{A}_6^{1-\rm loop}(1_q,2_{\bar{Q}},3_Q,4_{\bar{q}}) = 2e^2g^4\Big[\\
&\times\Big(-Q^q + v^e_{L,R}v^q_{L,R}\mathcal{P}_Z(s_{56})\Big)\Big[N_c\,\delta_{i_1}^{\bar{i}_2}\,\delta_{i_3}^{\bar{i}_4}\,A_{6;1}(1_q,2_{\bar{Q}},3_Q,4_{\bar{q}}) + \delta_{i_1}^{\bar{i}_4}\,\delta_{i_3}^{\bar{i}_2}\,A_{6;2}(1_q,2_{\bar{Q}},3_Q,4_{\bar{q}})\Big]\\
&+\Big(-Q^Q + v^e_{L,R}v^Q_{L,R}\mathcal{P}_Z(s_{56})\Big)\Big[N_c\,\delta_{i_1}^{\bar{i}_2}\,\delta_{i_3}^{\bar{i}_4}\,A_{6;1}(3_Q,4_{\bar{q}},1_q,2_{\bar{Q}}) + \delta_{i_1}^{\bar{i}_4}\,\delta_{i_3}^{\bar{i}_2}\,A_{6;2}(3_Q,4_{\bar{q}},1_q,2_{\bar{Q}})\Big]\\
&+\frac{v^e_{L,R}}{\sin 2\theta_W}\mathcal{P}_Z(s_{56})\left(\delta_{i_1}^{\bar{i}_2}\,\delta_{i_3}^{\bar{i}_4} - \frac{1}{N_c}\delta_{i_1}^{\bar{i}_4}\,\delta_{i_3}^{\bar{i}_2}\right)A_{6;3}(1_q,2_{\bar{Q}},3_Q,4_{\bar{q}})\Big]. \qquad \text{(B.3)}
\end{aligned}$$

For the case of identical quark flavours ($q = Q$) see ref. [36].

We are only concerned with the terms containing heavy quark loops. The formulas for the four-quark partial amplitudes, $A_{6;i}(1_q^+,2_{\bar{Q}}^{\pm},3_Q^{\mp},4_{\bar{q}}^-)$, expressed in terms of primitive amplitudes are

$$\begin{aligned}
A_{6;1}(1_q^+,2_{\bar{Q}}^+,3_Q^-,4_{\bar{q}}^-) &= A_6^{++}(1,2,3,4)\\
&\quad -\frac{2}{N_c^2}\big(A_6^{++}(1,2,3,4)+A_6^{+-}(1,3,2,4)\big)+\frac{1}{N_c^2}A_6^{\rm sl}(2,3,1,4)\\
&\quad +\frac{n_s-n_f}{N_c}A_6^{s,++}(1,2,3,4)-\frac{n_f}{N_c}A_6^{f,++}(1,2,3,4)+\frac{1}{N_c}A_6^{t,++}(1,2,3,4)\,,\\
A_{6;2}(1_q^+,2_{\bar{Q}}^+,3_Q^-,4_{\bar{q}}^-) &= A_6^{+-}(1,3,2,4)\\
&\quad +\frac{1}{N_c^2}\big(A_6^{+-}(1,3,2,4)+A_6^{++}(1,2,3,4)\big)-\frac{1}{N_c^2}A_6^{\rm sl}(2,3,1,4)\\
&\quad -\frac{n_s-n_f}{N_c}A_6^{s,++}(1,2,3,4)+\frac{n_f}{N_c}A_6^{f,++}(1,2,3,4)-\frac{1}{N_c}A_6^{t,++}(1,2,3,4)\,,\\
A_{6;3}(1_q^+,2_{\bar{Q}}^+,3_Q^-,4_{\bar{q}}^-) &= A_6^{\rm ax}(1,4,2,3)\,, \qquad \text{(B.4)}
\end{aligned}$$

and

$$\begin{aligned}
A_{6;1}(1_q^+,2_{\bar{Q}}^-,3_Q^+,4_{\bar{q}}^-) &= A_6^{+-}(1,2,3,4)\\
&\quad -\frac{2}{N_c^2}\big(A_6^{+-}(1,2,3,4)+A_6^{++}(1,3,2,4)\big)-\frac{1}{N_c^2}A_6^{\rm sl}(3,2,1,4)\\
&\quad +\frac{n_s-n_f}{N_c}A_6^{s,+-}(1,2,3,4)-\frac{n_f}{N_c}A_6^{f,+-}(1,2,3,4)+\frac{1}{N_c}A_6^{t,+-}(1,2,3,4)\,,
\end{aligned}$$

JHEP01(2017)020

$$A_{6;2}(1_q^+,2_{\bar{Q}}^-,3_Q^+,4_{\bar{q}}^-) = A_6^{++}(1,3,2,4)$$
$$+\frac{1}{N_c^2}\left(A_6^{++}(1,3,2,4)+A_6^{+-}(1,2,3,4)\right)+\frac{1}{N_c^2}A_6^{\rm sl}(3,2,1,4)$$
$$-\frac{n_s-n_f}{N_c}A_6^{s,+-}(1,2,3,4)+\frac{n_f}{N_c}A_6^{f,+-}(1,2,3,4)-\frac{1}{N_c}A_6^{t,+-}(1,2,3,4)\,,$$
$$A_{6;3}(1_q^+,2_{\bar{Q}}^-,3_Q^+,4_{\bar{q}}^-) = -A_6^{\rm ax}(1,4,3,2)\,. \tag{B.5}$$

B.3 Top loops — vacuum polarization contribution

The one-loop contribution to the unrenormalized vacuum polarization is given by,

$$\Gamma^{\mu\nu}(p) = ig^2 c_\Gamma\left[g^{\mu\nu}p^2 - p^\mu p^\nu\right]\pi(p^2)\,, \tag{B.6}$$

with c_Γ given in eq. (A.10). The contribution of a top quark loop to $\pi(p^2)$ is

$$\pi(p^2) = -\frac{4}{3}T_R\left[B_0(p,m,m)+\frac{2m^2}{p^2}[B_0(p,m,m)-B_0(0,m,m)]-\frac{1}{3}\right], \tag{B.7}$$

where $T_R=\frac{1}{2}$. Renormalization is effected by performing subtraction at zero momentum transfer ($p^2=0$), so that the effect of the top quark decouples at large momentum transfer. In this scheme both the running of the coupling and the evolution of the parton distributions remain in the five flavour scheme. We find

$$\pi(p^2)-\pi(0) = -\frac{2}{3}\left[\left(1+\frac{2m^2}{p^2}\right)[B_0(p,m,m)-B_0(0,m,m)]+\frac{1}{3}\right]. \tag{B.8}$$

In this subtraction scheme, the renormalized contribution coming from the diagrams shown in figure 3 is,

$$A_6^{t,+\pm}(1_q^+,2_{\bar{Q}}^+,3_Q^-,4_{\bar{q}}^+,5_{\bar{e}}^-,6_e^+) = -c_\Gamma\frac{2}{3}\left[\left(1+\frac{2m^2}{s_{23}}\right)(B_0(p_{23},m,m)-B_0(p_3,m,m))+\frac{1}{3}\right]$$
$$\times A_6^{\rm tree}(1_q^+,2_{\bar{Q}}^\pm,3_Q^\mp,4_{\bar{q}}^+,5_{\bar{e}}^-,6_e^+)\,. \tag{B.9}$$

Performing the large mass expansion, in the limit $m\to\infty$ we get,

$$A_6^{t,+\pm}(1_q^+,2_{\bar{Q}}^+,3_Q^-,4_{\bar{q}}^+,5_{\bar{e}}^-,6_e^+) = -c_\Gamma\left[\frac{2}{15}\frac{s_{23}}{m^2}+\frac{1}{70}\left(\frac{s_{23}}{m^2}\right)^2+\frac{2}{945}\left(\frac{s_{23}}{m^2}\right)^3+O\left(\left(\frac{s_{23}}{m^2}\right)^4\right)\right]$$
$$\times A_6^{\rm tree}(1_q^+,2_{\bar{Q}}^\pm,3_Q^\mp,4_{\bar{q}}^+,5_{\bar{e}}^-,6_e^+)\,. \tag{B.10}$$

This result agrees with BDK, eq. (12.2).

B.4 Top loops — axial vector coupling contribution

The contribution of the top and bottom quarks to the diagrams shown in figure 6 is,

$$A_6^{\rm ax}(1_q^+,2_{\bar{Q}}^-,3_Q,4_{\bar{q}}) = -2i\frac{1}{16\pi^2}\frac{1}{s_{56}} \tag{B.11}$$
$$\times\left[\left(\frac{[6\,3]\langle 4\,2\rangle\langle 2\,5\rangle}{\langle 1\,2\rangle}-\frac{[6\,1][1\,3]\langle 4\,5\rangle}{[1\,2]}\right)(f(m_t;s_{12},s_{34},s_{56})-f(m_b;s_{12},s_{34},s_{56}))\right.$$
$$\left.+\left(\frac{[6\,1]\langle 2\,4\rangle\langle 4\,5\rangle}{\langle 3\,4\rangle}-\frac{[6\,3][3\,1]\langle 2\,5\rangle}{[3\,4]}\right)(f(m_t;s_{34},s_{12},s_{56})-f(m_b;s_{34},s_{12},s_{56}))\right].$$

The axial triangle function f is presented in appendix F. In particular, the reduction of f to scalar integrals for the case at hand is given in eq. (F.10).

JHEP01(2017)020

C Six point amplitude, $A(1_q, 2_g, 3_g, 4_{\bar{q}}, 5_{\bar{e}}, 6_e)$

We now consider the process

$$0 \to q(p_1) + g(p_2) + g(p_3) + \bar{q}(p_4) + e^+(p_5) + e^-(p_6)\,, \tag{C.1}$$

where we have adopted the labelling convention of BDK for this case. The amplitudes for this process are most conveniently defined using the operation exch_{34}, which just represents the exchange of labels 3 and 4,

$$\mathrm{exch}_{34}: \quad 3 \leftrightarrow 4 \tag{C.2}$$

as well as the following "flip" functions:

$$\mathrm{flip}_1: \quad 1 \leftrightarrow 4, \quad 2 \leftrightarrow 3, \quad 5 \leftrightarrow 6, \quad \langle i\,j\rangle \leftrightarrow [i\,j]\,. \tag{C.3}$$

$$\mathrm{flip}_2: \quad 1 \leftrightarrow 2, \quad 3 \leftrightarrow 4, \quad 5 \leftrightarrow 6, \quad \langle ij\rangle \leftrightarrow [ij] \tag{C.4}$$

$$\mathrm{flip}_5: \quad 1 \leftrightarrow 2, \quad 5 \leftrightarrow 6, \quad \langle i\,j\rangle \leftrightarrow [i\,j]\,. \tag{C.5}$$

The latter symmetry operation is not defined in BDK, although it is a combination of exch_{34} (eq. (C.2)) and flip_2 (eq. (C.4)).

C.1 Tree graphs

Following ref. [15], the colour decomposition of the tree-level contribution to $\mathcal{A}_6$ is

$$\begin{aligned}\mathcal{A}_6^{\mathrm{tree}}(1_q, 2, 3, 4_{\bar{q}}) = {} & 2e^2g^2\big(-Q^q + v^e_{L,R}v^q_{L,R}\,\mathcal{P}_Z(s_{56})\big) \\ & \times \sum_{\sigma\in S_2} (T^{a_{\sigma(2)}}T^{a_{\sigma(3)}})_{i_1}^{\ \bar{\imath}_4}\ A_6^{\mathrm{tree}}(1_q, \sigma(2), \sigma(3), 4_{\bar{q}})\,.\end{aligned} \tag{C.6}$$

The independent results for helicities of the gluons in the tree amplitude are, cf. BDK eqs. (8.4), (8.9) and (8.15).

$$\begin{aligned}
&-iA_6^{\mathrm{tree}}(1_q^+, 2_g^+, 3_g^+, 4_{\bar{q}}^-) = -\frac{\langle 4\,5\rangle^2}{\langle 1\,2\rangle\langle 2\,3\rangle\langle 3\,4\rangle\langle 5\,6\rangle}\,, \\
&-iA_6^{\mathrm{tree}}(1_q^+, 2_g^+, 3_g^-, 4_{\bar{q}}^-) = \\
&\quad -\left[\frac{-\langle 3\,1\rangle[1\,2]\langle 4\,5\rangle\langle 3|(1{+}2)|6]}{\langle 1\,2\rangle s_{23}s_{123}s_{56}} + \frac{\langle 3\,4\rangle[4\,2][1\,6]\langle 5|(3{+}4)|2]}{[3\,4]s_{23}s_{234}s_{56}} + \frac{\langle 5|(3{+}4)|2]\langle 3|(1{+}2)|6]}{\langle 1\,2\rangle[3\,4]s_{23}s_{56}}\right], \\
&-iA_6^{\mathrm{tree}}(1_q^+, 2_g^-, 3_g^+, 4_{\bar{q}}^-) = \\
&\quad -\left[\frac{[1\,3]^2\langle 4\,5\rangle\langle 2|(1+3)|6]}{[1\,2]s_{23}s_{123}s_{56}} - \frac{\langle 2\,4\rangle^2[1\,6]\langle 5|(2+4)|3]}{\langle 3\,4\rangle s_{23}s_{234}s_{56}} - \frac{[1\,3]\langle 2\,4\rangle[1\,6]\langle 4\,5\rangle}{\langle 3\,4\rangle[1\,2]s_{23}s_{56}}\right].
\end{aligned} \tag{C.7}$$

The remaining helicity combination may be obtained by combining the operations of parity (interchanging $\langle i\,j\rangle$ and $[i\,j]$) and charge conjugation (exchanging identities of external fermions and anti-fermions). Thus we have,

$$A_6^{\mathrm{tree}}(1_q^+, 2_g^-, 3_g^-, 4_{\bar{q}}^-) = \mathrm{flip}_1\left[A_6^{\mathrm{tree}}(1_q^+, 2_g^+, 3_g^+, 4_{\bar{q}}^-)\right], \tag{C.8}$$

where the operation flip_1 is defined in eq. (C.3) (and also BDK eq. (6.7)).

C.2 General structure at one-loop

The one-loop colour decomposition is given by [15]

$$
\begin{aligned}
\mathcal{A}_6^{1-\text{loop}}(1_q,2,3,4_{\bar{q}}) = 2e^2\, g^4 \Bigg\{ & \left(-Q^q + v^e_{L,R} v^q_{L,R}\, \mathcal{P}_Z(s_{56})\right) \\
& \times \left[N_c \sum_{\sigma\in S_2} \left(T^{a_{\sigma(2)}} T^{a_{\sigma(3)}}\right)_{i_1}{}^{\bar{\imath}_4}\, A_{6;1}(1_q,\sigma(2),\sigma(3),4_{\bar{q}}) + \delta^{a_2 a_3}\, \delta_{i_1}{}^{\bar{\imath}_4}\, A_{6;3}(1_q,4_{\bar{q}};2,3) \right] \\
& + \sum_{f=1}^{n_f} \left(-Q^f + v^e_{L,R} v^f_V \mathcal{P}_Z(s_{56})\right) \\
& \qquad \times \left[\left(T^{a_2} T^{a_3}\right)_{i_1}{}^{\bar{\imath}_4} + \left(T^{a_3} T^{a_2}\right)_{i_1}{}^{\bar{\imath}_4} - \frac{2}{N_c}\, \delta^{a_2 a_3}\, \delta_{i_1}{}^{\bar{\imath}_4} \right] A^{\text{v}}_{6;4}(1_q,4_{\bar{q}};2,3) \\
& + \sum_{f=b,t} 2 v^f_A v^e_{L,R}\, \mathcal{P}_Z(s_{56}) \\
\times \Bigg[& \sum_{\sigma\in S_2} \left(\left(T^{a_{\sigma(2)}} T^{a_{\sigma(3)}}\right)_{i_1}{}^{\bar{\imath}_4} - \frac{1}{N_c} \delta^{a_2 a_3}\, \delta_{i_1}{}^{\bar{\imath}_4} \right) A^{\text{ax}}_{6;4}(1_q,4_{\bar{q}};\sigma(2),\sigma(3)) \\
& \qquad + \frac{1}{N_c} \delta^{a_2 a_3}\, \delta_{i_1}{}^{\bar{\imath}_4}\, A^{\text{ax}}_{6;5}(1_q,4_{\bar{q}};2,3) \Bigg] \Bigg\}\,,
\end{aligned}
\tag{C.9}
$$

where Q^i is the electric charge (in units of the positron charge) of the ith quark and n_f is the number of light quark flavours. The partial amplitudes $A_{6;1}$ and $A_{6;3}$ represent contributions where the Z couples to the fermion line as shown in figure 4. The partial amplitudes $A^{\text{v}}_{6;4}$, $A^{\text{ax}}_{6;4}$ and $A^{\text{ax}}_{6;5}$ represent the contributions from a photon or Z coupling to a fermion loop through a vector or axial-vector coupling. The full results with massless partons running in the loop have been given in BDK. The addition of this paper is to insert the full top quark mass dependence of $A_{6;1}, A^{\text{v}}_{6;4}$, $A^{\text{ax}}_{6;4}$ and $A^{\text{ax}}_{6;5}$.

The partial amplitudes were further decomposed in the original BDK paper into primitive amplitudes as follows:

$$
\begin{aligned}
A_{6;1}(1_q,2,3,4_{\bar{q}}) &= A_6(1_q,2,3,4_{\bar{q}}) - \frac{1}{N_c^2} A_6(1_q,4_{\bar{q}},3,2) \\
&\quad + \frac{n_s - n_f}{N_c} A^s_6(1_q,2,3,4_{\bar{q}}) - \frac{n_f}{N_c} A^f_6(1_q,2,3,4_{\bar{q}}) + \frac{1}{N_c} A^t_6(1_q,2,3,4_{\bar{q}})\,, \\
A_{6;3}(1_q,4_{\bar{q}};2,3) &= A_6(1_q,2,3,4_{\bar{q}}) + A_6(1_q,3,2,4_{\bar{q}}) + A_6(1_q,2,4_{\bar{q}},3) + A_6(1_q,3,4_{\bar{q}},2) \\
&\quad + A_6(1_q,4_{\bar{q}},2,3) + A_6(1_q,4_{\bar{q}},3,2)\,, \\
A^{\text{v}}_{6;4}(1_q,4_{\bar{q}};2,3) &= -A^{\text{v}s}_6(1_q,4_{\bar{q}},2,3) - A^{\text{v}f}_6(1_q,4_{\bar{q}},2,3)\,, \\
A^{\text{ax}}_{6;4}(1_q,4_{\bar{q}};2,3) &= A^{\text{ax}}_6(1_q,4_{\bar{q}},2,3)\,, \\
A^{\text{ax}}_{6;5}(1_q,4_{\bar{q}};2,3) &= A^{\text{ax,sl}}_6(1_q,4_{\bar{q}},2,3)\,.
\end{aligned}
\tag{C.10}
$$

We must therefore provide new expressions, containing the full top quark mass dependence, for the following quantities:

- $A^t_6(1_q,2,3,4_{\bar{q}})$, in which the Z boson couples to the light quark line.

JHEP01(2017)020

- $A^{\rm v}_{6;4}(1_q, 4_{\bar q}; 2, 3)$, in which the Z boson is radiated from a quark loop through the vector coupling. In our approach it is not useful to perform an additional decomposition into $A^{{\rm v}s}_6$ and $A^{{\rm v}f}_6$.

- $A^{\rm ax}_6(1_q, 4_{\bar q}, 2, 3)$ and $A^{\rm ax,sl}_6(1_q, 4_{\bar q}, 2, 3)$, where the Z boson is radiated from a top or bottom quark loop through the axial coupling.

For the quantities $A^{\rm v}_{6;4}$, $A^{\rm ax}_6$ and $A^{\rm ax,sl}_6$ we will follow the conventions of the original BDK paper and not present expressions for the momentum labelling as in eq. (C.10), but instead do so for the configuration $(1_q, 2_{\bar q}; 3, 4)$.

The colour sum for $e^+ e^- \to \bar q q g g g$ in terms of partial amplitudes is,

$$\begin{aligned}
\sum_{\rm colors} [\mathcal{A}^*_6 \mathcal{A}_6]_{\rm NLO} \;=\; & 8 e^4 g^6 (N_c^2 - 1) {\rm Re} \Bigg\{ \Big(-Q^q + v^e_{L,R} v^q_{L,R} \mathcal{P}^*_Z(s_{56})\Big) A^{\rm tree*}_6(1_q, 2, 3, 4_{\bar q}) \\
& \times \Bigg[\Big(-Q^q + v^e_{L,R} v^q_{L,R} \mathcal{P}_Z(s_{56})\Big) \big[(N_c^2 - 1) A_{6;1}(1_q, 2, 3, 4_{\bar q}) \\
& \qquad - A_{6;1}(1_q, 3, 2, 4_{\bar q}) + A_{6;3}(1_q, 4_{\bar q}; 2, 3) \big] \\
& + \sum_{f=1}^{n_f} \Big(-Q^f + v^e_{L,R} v^f_V \mathcal{P}_Z(s_{56})\Big) \left(N_c - \frac{4}{N_c} \right) A^{\rm v}_{6;4}(1_q, 4_{\bar q}; 2, 3) \\
& + \sum_{f=t,b} 2 v^e_{L,R} v^f_A \mathcal{P}_Z(s_{56}) \Bigg[\left(N_c - \frac{2}{N_c} \right) A^{\rm ax}_{6;4}(1_q, 4_{\bar q}; 2, 3) - \frac{2}{N_c} A^{\rm ax}_{6;4}(1_q, 4_{\bar q}; 3, 2) \\
& + \frac{1}{N_c} A^{\rm ax}_{6;5}(1_q, 4_{\bar q}; 2, 3) \Bigg] \Bigg] \Bigg\} \;+\; \{2 \leftrightarrow 3\} \,. \qquad \text{(C.11)}
\end{aligned}$$

C.3 Result for $\mathcal{A}^t_6(1_q, 2, 3, 4_{\bar q})$

The aim of this section is to calculate the full mass dependence of the quantity A^t_6, which is part of $A_{6;1}$ that is defined in eq. (C.10). The relevant diagrams do not contribute to $A_{6;3}$. The minus sign for the fermion loop is included in A^t_6. For this case the only non-zero amplitudes occur when the gluons have the same helicity.

The amplitude can be written as

$$\mathcal{A}^t_6(1_q, 2^+, 3^+, 4_{\bar q}) = \mathcal{A}^s_6(1_q, 2^+, 3^+, 4_{\bar q}) \times F^t(s_{23}, m^2) \,, \qquad \text{(C.12)}$$

where

$$\mathcal{A}^s_6(1_q, 2^+, 3^+, 4_{\bar q}) = i \frac{c_\Gamma}{3} \frac{1}{\langle 2\,3\rangle^2 s_{56}} \left[- \frac{\langle 4\,5\rangle [6|(1+2)|3\rangle [3\,1]}{s_{123}} + \frac{[1\,6] \langle 5|(4+2)|3] \langle 3\,4\rangle}{s_{234}} \right] . \qquad \text{(C.13)}$$

This agrees with BDK eq. (8.2). The function $\mathcal{A}^s_6$ is anti-symmetric under the exchange of 2 and 3. The mass-dependence enters through the function

$$F^t(s_{23}, m^2) = - \left[1 + 6 m^2 C_0(p_2, p_3, m, m, m) + \frac{12 m^2}{s_{23}} \Big(B_0(p_{23}, m, m) - B_0(p_2, m, m) \Big) \right] , \qquad \text{(C.14)}$$

JHEP01(2017)020

which accounts for the effect of vertex and bubble corrections such as those shown in figure 4. In our renormalization scheme there is no net effect from top-quark self-energy corrections on external gluons. The large mass expansion of $F^t(s,m^2)$ is

$$F^t(s,m^2) = \frac{1}{20}\frac{s}{m^2} + \frac{1}{210}\left(\frac{s}{m^2}\right)^2 + \frac{1}{1680}\left(\frac{s}{m^2}\right)^3 + O\left(\left(\frac{s}{m^2}\right)^4\right). \tag{C.15}$$

After using this expansion the result for A_6^t agrees with BDK eq. (8.3).

C.4 Result for $\mathcal{A}^{\rm v}_{6;4}(1_q, 2_{\bar{q}}, 3, 4)$

The result for loops of massless quarks that couple via a vector coupling have been given in BDK, in particular through their eqs. (11.1-11.2) and eqs. (11.5-11.7). In their approximation, which retains only terms of order $1/m_t^2$, the top quark loop does not contribute since it enters only at order $1/m_t^4$ and beyond. We therefore introduce the extra contribution of the top quark loop through,

$$\mathcal{A}^{\rm v}_{6;4}(1_q, 2_{\bar{q}}, 3, 4) = \mathcal{A}^{{\rm v},BDK}_{6;4}(1_q, 2_{\bar{q}}, 3, 4) + \mathcal{A}^{{\rm v},t}_{6;4}(1_q, 2_{\bar{q}}, 3, 4)\,. \tag{C.16}$$

We will not present explicit results for the term $\mathcal{A}^{{\rm v},t}_{6;4}$ since they can be simply related to previously published results for the process $gg \to ZZ$ [37]. This exploits the fact that $\mathcal{A}^{{\rm v},t}_{6;4}$ only receives contributions from box (not triangle) diagrams, so that replacing a single $Z \to \ell\bar{\ell}$ current by a $g^* \to q\bar{q}$ one is trivial. We have,

$$\mathcal{A}^{{\rm v},t}_{6;4}(1_q, 2_{\bar{q}}, 3, 4) = -\left[A_{LL}(3_g, 4_g, 1_e, 2_{\bar{e}}, 6_\mu, 5_{\bar{\mu}}) + A_{LR}(3_g, 4_g, 1_e, 2_{\bar{e}}, 6_\mu, 5_{\bar{\mu}})\right]. \tag{C.17}$$

This is in accord with the procedure for extracting the vector-vector contribution given in eq. (24) of ref. [37], up to an expected change in the overall factor and a sign to match the conventions of BDK.

C.5 Result for $A^{\rm ax,sl}(1_q, 2_{\bar{q}}, 3_g, 4_g)$

The sub-leading colour piece receives contributions from the diagram of the type shown in figure 5a. The full result for the third generation isodoublet is

$$-iA^{\rm ax,sl}(1_q^+, 2_{\bar{q}}^-, 3_g^+, 4_g^+) = c_\Gamma \frac{\langle 2\,5\rangle[4\,6]\langle 2|(1+3)|4]}{\langle 1\,3\rangle\langle 2\,3\rangle s_{56}}\left[2f(m_t;0,s_{123},s_{56}) - \frac{L_1(\frac{-s_{123}}{-s_{56}})}{s_{56}}\right] + {\rm exch}_{34}\,, \tag{C.18}$$

where exch_{34} is defined in eq. (C.2). This expression agrees with BDK eq. (11.4). The result when the gluons have opposite helicities is,

$$-iA_6^{\rm ax,sl}(1_q^+, 2_{\bar{q}}^-, 3_g^+, 4_g^-) = c_\Gamma \frac{\langle 2\,4\rangle\langle 4\,5\rangle\langle 2|(1+3)|6]}{\langle 1\,3\rangle\langle 2\,3\rangle s_{56}}\left[2f(m_t;0,s_{123},s_{56}) - \frac{L_1(\frac{-s_{123}}{-s_{56}})}{s_{56}}\right] + {\rm flip}_2\,. \tag{C.19}$$

The function L_1 is defined in eq. (A.15) and f is defined in eq. (F.5). The swap flip_2 is defined in eq. (C.4).

$$A_6^{\rm ax,sl}(1_q^+, 2_{\bar{q}}^-, 3_g^-, 4_g^+) = A_6^{\rm ax,sl}(1_q^+, 2_{\bar{q}}^-, 3_g^+, 4_g^-)|_{3\leftrightarrow 4}\,. \tag{C.20}$$

This agrees with BDK eq. (11.12).

C.6 Result for $A^{\rm ax}(1_q, 2_{\bar{q}}, 3_g, 4_g)$

The most complicated case in which to account for the top-quark mass is the calculation of the leading-colour contribution from a loop of massive fermions with an axial vector coupling to the Z-boson. For a complete isodoublet of massless quarks there is no net contribution of this type since the diagrams precisely cancel between the isospin partners. For the (t, b) isodoublet this is no longer the case once a non-zero mass for the top quark is assumed. The contribution of this isodoublet has been presented, retaining only the leading $1/m_t^2$ terms in an expansion of the top-quark diagrams, in the paper of BDK. The result for the massless diagrams can be extracted from their eqs. (11.3)-(11.4) and eqs. (11.8)-(11.12), simply by discarding the terms proportional to $1/m_t^2$.

Our base amplitude can be written as follows,

$$-iA_6^{\rm ax}(1_q^+, 2_{\bar{q}}^-, 3_g^{h_3}, 4_g^{h_4}, 5_{\bar{e}}^-, 6_e^+) = \sum_{x,y,z} d_{x|y|z}(3^{h_3}, 4^{h_4}) D_0^{x|y|z} + \sum_{x,y} c_{x|y}(3^{h_3}, 4^{h_4}) C_0^{x|y} + \sum_x b_x(3^{h_3}, 4^{h_4}) B_0^x + R(3^{h_3}, 4^{h_4})\,. \tag{C.21}$$

This is an expansion in terms of the scalar box ($D_0^{x|y|z}$), triangle ($C_0^{x|y}$) and bubble (B_0^x) integrals, defined explicitly in appendix D, as well as a left-over rational part (R). The box and triangle coefficients in that expansion have a further mass expansion,

$$d_{x|y|z}(3^{h_3}, 4^{h_4}) = d^{(0)}_{x|y|z}(3^{h_3}, 4^{h_4}) + m^2 d^{(2)}_{x|y|z}(3^{h_3}, 4^{h_4})\,, \tag{C.22}$$

$$c_{x|y}(3^{h_3}, 4^{h_4}) = c^{(0)}_{x|y}(3^{h_3}, 4^{h_4}) + m^2 c^{(2)}_{x|y}(3^{h_3}, 4^{h_4})\,, \tag{C.23}$$

while the bubble coefficients and rational part are independent of the mass m. We use this feature to simplify the presentation of our results by replacing the expansion of eq. (C.21) by the more compact form,

$$\begin{aligned} -iA_6^{\rm ax}(1_q^+, 2_{\bar{q}}^-, 3_g^{h_3}, 4_g^{h_4}, 5_{\bar{e}}^-, 6_e^+) &= -iA^{\rm ax}_{6,BDK}(1_q^+, 2_{\bar{q}}^-, 3_g^{h_3}, 4_g^{h_4}, 5_{\bar{e}}^-, 6_e^+) \\ &+ d_{3|12|4}(3^{h_3}, 4^{h_4}) D_0^{3|12|4} + d_{4|3|12}(3^{h_3}, 4^{h_4}) D_0^{4|3|12} + d_{3|4|12}(3^{h_3}, 4^{h_4}) D_0^{3|4|12} \\ &+ c_{3|4}(3^{h_3}, 4^{h_4}) C_0^{3|4} + c_{12|3}(3^{h_3}, 4^{h_4}) C_0^{12|3} + c_{12|4}(3^{h_3}, 4^{h_4}) C_0^{12|4} \\ &+ c_{3|124}(3^{h_3}, 4^{h_4}) C_0^{3|124} + c_{4|123}(3^{h_3}, 4^{h_4}) C_0^{4|123} + c^{(2)}_{12|34}(3^{h_3}, 4^{h_4}) C_0^{12|34}\,. \end{aligned} \tag{C.24}$$

The function $A^{\rm ax}_{6,BDK}$ collects the bubble and rational terms as well as the contribution from the triangle coefficient $c^{(0)}_{12|34}$, all of which may be extracted from the previous calculation of BDK. In the paper of BDK, the bubble coefficients have been re-organized to perform cut completion, leading to more compact expressions. It is thus more efficient to use this compact form as our point of departure in presenting the results. Note though that, in our case, the relevant completed functions will be replaced by combinations of scalar bubble integrals that involve the internal top-quark mass. This is a consequence of the fact that the bubble coefficients are unchanged in the massive case, but the integrals themselves are changed.

Apart from the contribution that can be extracted from the results of BDK, eq. (C.24) also enumerates all of the remaining box and triangle integral coefficients that must be

JHEP01(2017)020

specified to complete the amplitudes. Although it appears that we should specify three box integral coefficients and six triangle coefficients this is not the case. A number of relations between the various coefficients can be used to minimize the number of independent expressions that must be given explicitly. The simplest relations are those that just correspond to a relabelling of momenta, for example,

$$d_{4|3|12}(3_g^{h_3}, 4_g^{h_4}) = -d_{3|4|12}(4_g^{h_4}, 3_g^{h_3})\,. \tag{C.25}$$

An additional simplification is due to the structure of the infrared divergences that are present when $m = 0$, which requires that the box and triangle coefficients are related. Explicitly, we make use of the identities,

$$c^{(0)}_{3|4}(3_g^{h_3}, 4_g^{h_4}) = -\frac{d^{(0)}_{4|3|12}(3_g^{h_3}, 4_g^{h_4})}{s_{123}} - \frac{d^{(0)}_{3|4|12}(3_g^{h_3}, 4_g^{h_4})}{s_{124}}\,, \tag{C.26}$$

and

$$c^{(0)}_{123|4}(3_g^{h_3}, 4_g^{h_4}) = (s_{56} - s_{123}) \left[\frac{d^{(0)}_{4|3|12}(3_g^{h_3}, 4_g^{h_4})}{s_{34}s_{123}} - \frac{d^{(0)}_{3|4|12}(3_g^{h_3}, 4_g^{h_4})}{s_{34}s_{124}} - \frac{c^{(0)}_{12|4}(3_g^{h_3}, 4_g^{h_4})}{s_{124} - s_{12}} \right], \tag{C.27}$$

together with the partner relation that can be obtained by exchanging labels 3 and 4. The coefficients of the m^2 term in the triangle expansion of eq. (C.23), i.e. $c^{(2)}_{x|y}$, are related to the rational part, R [25].[2] We exploit this relation in order to determine the coefficient $c^{(2)}_{12|34}$ which would normally require much simplification in an explicit analytic calculation,

$$c^{(2)}_{12|34}(3_g^{h_3}, 4_g^{h_4}) = 2R(3_g^{h_3}, 4_g^{h_4}) - c^{(2)}_{123|4}(3_g^{h_3}, 4_g^{h_4}) - c^{(2)}_{124|3}(3_g^{h_3}, 4_g^{h_4})\,. \tag{C.28}$$

Explicit results for the remaining independent coefficients will be given below.

C.6.1 Box coefficients

For the box coefficients $d^{(i)}$ it is sufficient to consider only 3^+4^+ and 3^+4^- helicity combinations. The remaining helicities are obtained from these ones according to,

$$d^{(i)}(3^-, 4^-) = -\text{flip}_5\left[d^{(i)}(3^+, 4^+)\right], \qquad d^{(i)}(3^-, 4^+) = -\text{flip}_5\left[d^{(i)}(3^+, 4^-)\right], \tag{C.29}$$

where flip_5 is defined in eq. (C.5).

[2] This relation would normally also involve the m^4 terms in the expansion of the box integral coefficients, but they vanish in this case.

JHEP01(2017)020

$d_{3|12|4}$ coefficients. The coefficients of the box integrals with gluons situated on opposite corners are:

$$d^{(0)}_{3|12|4}(3^+,4^+) = \frac{(s_{123}s_{124}-s_{12}s_{56})(\langle 2\,3\rangle\langle 4\,5\rangle+\langle 2\,4\rangle\langle 3\,5\rangle)\langle 2\,5\rangle}{4\langle 1\,2\rangle\langle 3\,4\rangle^3\langle 5\,6\rangle} \tag{C.30}$$

$$\begin{aligned} d^{(2)}_{3|12|4}(3^+,4^+) = \frac{1}{2s_{12}s_{56}\langle 3\,4\rangle^3}\Bigg[&\langle 2\,3\rangle^2\langle 4\,5\rangle\Big(\langle 4|(1+2)|4][1\,6][2\,3]-\langle 4|(2+3)|6][1\,2][3\,4]\Big)\\ &+\frac{1}{2}\langle 2\,3\rangle\langle 4|(1+2)|3]\Big(\langle 3\,4\rangle\langle 4\,5\rangle[1\,4][4\,6]+\langle 3\,4\rangle\langle 3\,5\rangle[1\,4][3\,6]\\ &-\langle 4|(1+2)|4]\langle 3\,5\rangle[1\,6]-\langle 3\,4\rangle\langle 2\,5\rangle[1\,2][4\,6]-2\langle 2\,3\rangle\langle 4\,5\rangle[1\,6][2\,4]\Big)\\ &+\frac{1}{2}\langle 2\,3\rangle\langle 4\,5\rangle[1\,6]\langle 3|(1+2)|4]\langle 4|(1+2)|3]\Bigg]-\Big[3\leftrightarrow 4\Big], \end{aligned} \tag{C.31}$$

$$d^{(0)}_{3|12|4}(3^+,4^-) = 0\,, \tag{C.32}$$

$$\begin{aligned} d^{(2)}_{3|12|4}(3^+,4^-) = \frac{1}{2s_{12}s_{34}s_{56}[3\,4]}\Bigg[&-[1\,3][3\,4]^2[3\,6]\langle 2\,4\rangle\langle 3\,4\rangle\langle 4\,5\rangle\\ &-\frac{\langle 4|(1+2)|3]}{2\,\langle 3|(1+2)|4]}\Big([1\,3]^2[1\,4][4\,6]\langle 2\,5\rangle\langle 1\,3\rangle\langle 1\,4\rangle+[2\,3][1\,4]\langle 5|(2+4)|3][4\,6]\langle 2\,4\rangle\langle 2\,3\rangle\\ &-[1\,3][1\,4][3\,4]\langle 2|(1+3)|6](\langle 1\,3\rangle\langle 4\,5\rangle-\langle 1\,5\rangle\langle 3\,4\rangle)\\ &-[1\,3][1\,4][4\,6]\langle 1|(2+4)|3]\langle 2\,3\rangle\langle 4\,5\rangle+[2\,3][1\,4][3\,6]\langle 2|(1+3)|4]\langle 2\,4\rangle\langle 3\,5\rangle\\ &+2[1\,4][3\,6]\langle 4\,5\rangle\langle 3|(2+4)|3]\langle 2|(1+3)|4]-2[2\,1][3\,4][1\,3][4\,6]\langle 2\,4\rangle\langle 2\,5\rangle\langle 1\,3\rangle\Big)\\ &-\frac{\langle 4|(1+2)|3]}{2}\Big([1\,3]^2[4\,6]\langle 2\,4\rangle\langle 1\,5\rangle-[1\,3][1\,4][3\,6]\langle 2\,1\rangle\langle 4\,5\rangle-2[1\,3][3\,4][3\,6]\langle 2\,3\rangle\langle 4\,5\rangle\\ &+\langle 5|(2+3)|1][3\,4][3\,6]\langle 2\,4\rangle+[1\,3][4\,6]\langle 2\,4\rangle\langle 5|(2+4)|3]\Big)\Bigg]. \end{aligned} \tag{C.33}$$

$d_{3|4|12}$ coefficients. The box integrals corresponding to two contiguous gluons have the following coefficients:

$$d^{(0)}_{3|4|12}(3^+,4^+) = 0\,, \tag{C.34}$$

$$d^{(2)}_{3|4|12}(3^+,4^+) = \frac{\langle 2\,5\rangle[1\,2][3\,4]}{2\langle 3\,4\rangle s_{12}s_{56}}\left[\langle 2\,3\rangle[3\,6]-\langle 2|(1+4)|6]-\frac{s_{124}\langle 2\,3\rangle[6\,4]}{\langle 3|(1+2)|4]}-\frac{s_{124}\langle 2\,4\rangle[6\,3]}{\langle 4|(1+2)|3]}\right], \tag{C.35}$$

$$d^{(0)}_{3|4|12}(3^+,4^-) = \frac{1}{4}s_{34}s_{124}\left[\frac{\langle 3|(2+4)|1]^2\langle 5|(1+2)|4]^2-[1\,4]^2\langle 3\,5\rangle^2 s_{124}^2}{[2\,1]\langle 6\,5\rangle\langle 3|(1+2)|4]^4}\right], \tag{C.36}$$

$$\begin{aligned} d^{(2)}_{3|4|12}(3^+,4^-) = &\frac{\langle 2\,4\rangle s_{124}}{2\langle 3|(1+2)|4]s_{12}s_{56}}\Big([2\,1][3\,6]\langle 2\,5\rangle+[1\,3][6\,4]\langle 4\,5\rangle\Big)\\ &+3\frac{s_{124}\langle 2\,3\rangle\langle 4|(1+2)|3][4\,6]\langle 5|(2+4)|1]}{2\langle 3|(1+2)|4]^2 s_{12}s_{56}}\\ &+\frac{\langle 4|(1+2)|3]}{2\langle 3|(1+2)|4]s_{12}s_{56}}\Big(\langle 5|(2+4)|1]([3\,6]\langle 2\,3\rangle-[4\,6]\langle 2\,4\rangle)-[1\,6]\langle 2\,5\rangle s_{124}\\ &+[1\,4][3\,6]\langle 2\,4\rangle\langle 3\,5\rangle\Big)-\frac{[1\,3][3\,6]\langle 2\,4\rangle\langle 4\,5\rangle}{2s_{12}s_{56}}\,. \end{aligned} \tag{C.37}$$

JHEP01(2017)020

Coefficient	$c^{(0)}$	$c^{(2)}$
$c_{12\|34}$	extracted from BDK	rational relation, eq. (C.28)
$c_{12\|3}$	Section C.6.2	vanishes
$c_{12\|4}$	Section C.6.2+eq. (C.25) relabelling	vanishes
$c_{4\|123}$	infrared relation, eq. (C.27)	Section C.6.2
$c_{3\|124}$	infrared relation, eq. (C.27)	Section C.6.2+eq. (C.25) relabelling
$c_{3\|4}$	infrared relation, eq. (C.26)	vanishes

Table 2. Determination of triangle coefficients.

C.6.2 Triangle coefficients

In general there are six possible kinematic configurations of triangle integrals that may contribute to this partial amplitude. These are:

$$c_{3|4}, \quad c_{12|3}, \quad c_{12|4}, \quad c_{12|34}, \quad c_{4|123}, \quad c_{3|124}, \tag{C.38}$$

where the third leg is clear from momentum conservation. A summary of the method for determining each of these coefficients is shown in table 2. Note that, since the box integral coefficients $d^{(0)}_{3|4|12}$ and $d^{(0)}_{4|3|12}$ vanish in the same-sign helicity amplitudes, the infrared relation of eq. (C.26) implies that $c^{(0)}_{3|4}(3^{\pm}, 4^{\pm}) = 0$. The only coefficients that remain to be given explicitly are $c^{(0)}_{12|3}$ and $c^{(2)}_{4|123}$, which will be specified in sections C.6.2 and C.6.2 respectively below.

$c_{12|3}$ coefficients. For the triangle coefficients $c_{12|3}$ it is sufficient to consider only 3^+4^+ and 3^+4^- helicity combinations. The remaining helicities are obtained from these ones according to,

$$c_{12|3}(3^-, 4^-) = -\text{flip}_5\left[c_{12|3}(3^+, 4^+)\right], \qquad c_{12|3}(3^-, 4^+) = -\text{flip}_5\left[c_{12|3}(3^+, 4^-)\right], \tag{C.39}$$

where flip_5 is defined in eq. (C.5). As indicated in table 2, the mass-dependent terms in the coefficient vanish:

$$c^{(2)}_{12|3}(3^+, 4^+) = c^{(2)}_{12|3}(3^+, 4^-) = 0\,. \tag{C.40}$$

These triangle coefficients are thus fully-specified by,

$$\begin{aligned} c^{(0)}_{12|3}(3^+, 4^+) = &-\frac{1}{2}\frac{(s_{123} - s_{12})[1\,2][3\,4]}{\langle 3\,4\rangle^2 s_{12} s_{56}} \\ &\times\Big[\langle 2\,4\rangle^2\langle 3\,5\rangle[4\,6] + \langle 2\,3\rangle\langle 4\,5\rangle\langle 2|(1+3)|6] + \langle 2\,4\rangle\langle 2\,5\rangle\langle 3|(1+2)|6]\Big], \end{aligned} \tag{C.41}$$

$$\begin{aligned} c^{(0)}_{12|3}(3^+, 4^-) = &\Big(\langle 3|(1+2)|6]\langle 5|(3+4)|1]\langle 1\,2\rangle[1\,2]\Big(-\langle 1\,2\rangle[1\,4] + 2\langle 2\,3\rangle[3\,4]\Big) \\ &-\langle 3|(1+2)|6]\langle 2\,3\rangle^2\langle 4\,5\rangle[1\,2][3\,4]^2 + 2\langle 5|(1+2)|3]\langle 2\,3\rangle^2[1\,2][4\,6]\langle 2|(1+3)|2] \\ &+\langle 5|(3+4)|1]\langle 2\,3\rangle^2[1\,2]\Big(\langle 1\,2\rangle[2\,3][4\,6] + \langle 1\,3\rangle[3\,4][3\,6]\Big) \end{aligned}$$

JHEP01(2017)020

$$
\begin{aligned}
&+\langle 1\,2\rangle^3\langle 3\,5\rangle[1\,2]^2[1\,4][1\,6] + \langle 1\,2\rangle^2\langle 2\,3\rangle\langle 2\,5\rangle[1\,2]^3[4\,6]\\
&-3\langle 1\,2\rangle^2\langle 2\,3\rangle\langle 3\,5\rangle[1\,2]^2[1\,6][3\,4] + 3\langle 1\,2\rangle\langle 2\,3\rangle^2\langle 3\,5\rangle[1\,2]^2[3\,4][3\,6]\\
&-\langle 1\,2\rangle\langle 2\,3\rangle^2\langle 4\,5\rangle[1\,2][1\,4][2\,3][4\,6] + \langle 1\,3\rangle\langle 1\,5\rangle\langle 2\,3\rangle^2[1\,2][1\,3]^2[4\,6]\\
&-\langle 1\,3\rangle\langle 2\,3\rangle^2\langle 4\,5\rangle[1\,2][1\,4][3\,4][3\,6] - \langle 2\,3\rangle^3\langle 2\,5\rangle[1\,2][2\,3]^2[4\,6]\\
&+\langle 2\,3\rangle^3\langle 3\,5\rangle[1\,2][2\,3][3\,4][3\,6]\Big)\frac{s_{34}(s_{123}-s_{12})}{\langle 3|(1+2)|4]^3}\,.
\end{aligned}
\tag{C.42}
$$

$c_{4|123}$ coefficients. There are no simple symmetry relations between the $c_{4|123}$ coefficients of different helicities. We must therefore specify them all.

The coefficients that appear in the $m \to 0$ limit are simply obtained by using the infrared relation, eq. (C.27). The $c^{(2)}$ coefficients are more complicated:

$$
\begin{aligned}
&c^{(2)}_{4|123}(3_g^+,4_g^+) = \Big[\\
&\times 2\frac{\langle 3\,4\rangle[1\,3][4\,6]}{s_{123}}\Big(2\langle 1\,2\rangle\langle 2\,5\rangle[1\,2] - \langle 1\,5\rangle\langle 2\,4\rangle[1\,4] - \langle 2\,4\rangle\langle 3\,5\rangle[3\,4] + 2\langle 2\,5\rangle\langle 3\,4\rangle[3\,4]\Big)\\
&-4\frac{\langle 2|(5+6)|4]\langle 4|(5+6)|3]}{\langle 4|(5+6)|4]s_{123}}\Big(\langle 2\,5\rangle\langle 3\,4\rangle[1\,2][4\,6]\Big)\\
&-4\frac{\langle 2|(5+6)|4]}{\langle 1\,3\rangle\langle 4|(5+6)|4]s_{123}}\Big(\langle 1\,2\rangle\langle 1\,5\rangle\langle 2\,4\rangle\langle 3\,4\rangle[1\,2]^2[4\,6]\Big)\\
&+\frac{\langle 2|(5+6)|4]}{\langle 3|(5+6)|4]}\langle 3\,4\rangle[4\,6]\Big(\langle 4\,5\rangle[1\,4] - \langle 2\,5\rangle[1\,2]\Big)\\
&+\frac{\langle 2|(5+6)|4]}{\langle 4|(5+6)|3]}\Big(\langle 4\,5\rangle^2[1\,3][5\,6]\Big) + 4\frac{\langle 3|(5+6)|4]}{\langle 1\,3\rangle\langle 4|(5+6)|4]s_{123}}\Big(\langle 1\,2\rangle\langle 2\,4\rangle\langle 2\,5\rangle\langle 3\,4\rangle[1\,2][2\,3][4\,6]\Big)\\
&+\frac{\langle 4|(5+6)|1]}{\langle 4|(5+6)|3]}\Big(\langle 1\,2\rangle\langle 4\,5\rangle[1\,3][4\,6]\Big) + \frac{\langle 4|(5+6)|4]}{\langle 3|(5+6)|4]}\langle 3\,5\rangle[1\,4]\Big(2\langle 2\,4\rangle[4\,6] + \langle 2\,5\rangle[5\,6]\Big)\\
&-2\frac{\langle 4|(5+6)|4]}{\langle 4|(5+6)|3]}\Big(\langle 2\,4\rangle\langle 4\,5\rangle[1\,3][4\,6]\Big) - 4\frac{\langle 1\,2\rangle\langle 3\,4\rangle\langle 5\,6\rangle[1\,2][4\,6]}{\langle 1\,3\rangle\langle 4|(5+6)|4]s_{123}}\Big(\langle 1\,2\rangle\langle 2\,4\rangle[1\,2][4\,6]\Big)\\
&-4\frac{\langle 1\,2\rangle\langle 2\,5\rangle\langle 3\,4\rangle[1\,2][4\,6]\langle 4|(1+3)|4]}{\langle 1\,3\rangle\langle 4|(5+6)|4]} + 4\frac{\langle 1\,2\rangle\langle 2\,5\rangle\langle 3\,4\rangle[1\,2][4\,6]}{\langle 1\,3\rangle} - 2\frac{\langle 2\,3\rangle\langle 4\,5\rangle[1\,4][4\,6]}{\langle 3|(5+6)|4]}s_{123}\\
&-\frac{s_{123}}{\langle 3|(5+6)|4]\langle 4|(5+6)|4]}\Big(\langle 2\,4\rangle\langle 3\,4\rangle\langle 5\,6\rangle[1\,4][4\,6]^2\Big) + \frac{\langle 2\,4\rangle\langle 5\,6\rangle[4\,6]^2}{\langle 3|(5+6)|4]}\Big(\langle 3\,4\rangle[1\,4] - \langle 2\,3\rangle[1\,2]\Big)\\
&-\frac{s_{123}}{\langle 4|(5+6)|3]}\Big(\langle 2\,4\rangle\langle 4\,5\rangle[1\,6][3\,4]\Big) + \frac{s_{123}}{\langle 4|(5+6)|3]\langle 4|(5+6)|4]}\Big(\langle 2\,4\rangle\langle 4\,5\rangle^2[1\,4][3\,4][5\,6]\Big)\\
&+\frac{\langle 4\,5\rangle[5\,6]}{\langle 4|(5+6)|3]}\Big(\langle 1\,2\rangle\langle 4\,5\rangle[1\,3][1\,4] + 2\langle 2\,4\rangle\langle 2\,5\rangle[1\,2][3\,4]\\
&\quad -\langle 2\,4\rangle\langle 3\,5\rangle[1\,3][3\,4] - \langle 2\,5\rangle\langle 3\,4\rangle[1\,3][3\,4]\Big)\\
&+2\frac{\langle 3\,4\rangle\langle 5\,6\rangle[1\,3][4\,6]}{\langle 4|(5+6)|4]s_{123}}\Big(\langle 1\,3\rangle\langle 2\,4\rangle[1\,3][4\,6] - \langle 1\,2\rangle\langle 2\,4\rangle[1\,4][2\,6] - \langle 1\,4\rangle\langle 2\,4\rangle[1\,4][4\,6]\\
&\quad +\langle 2\,3\rangle\langle 2\,4\rangle[2\,6][3\,4] - 2\langle 1\,2\rangle\langle 3\,4\rangle[1\,4][3\,6] - 2\langle 1\,4\rangle\langle 2\,3\rangle[1\,3][4\,6]\\
&\quad +2\langle 2\,3\rangle\langle 3\,4\rangle[3\,4][3\,6] + \langle 2\,4\rangle\langle 3\,4\rangle[3\,4][4\,6]\Big)
\end{aligned}
$$

JHEP01(2017)020

$$+4\frac{\langle 2\,4\rangle\langle 4\,5\rangle[1\,4][4\,6]}{\langle 4|(5+6)|4]}s_{123}+\frac{[4\,6]}{\langle 4|(5+6)|4]}\Big(4\langle 1\,4\rangle\langle 2\,5\rangle\langle 3\,4\rangle[1\,3][1\,4]+2\langle 2\,4\rangle^2\langle 5\,6\rangle[1\,2][4\,6]$$
$$-2\langle 2\,4\rangle\langle 2\,5\rangle\langle 3\,4\rangle[1\,2][3\,4]+2\langle 2\,4\rangle\langle 2\,5\rangle\langle 3\,4\rangle[1\,4][2\,3]\Big)$$
$$+\langle 2\,4\rangle\langle 2\,5\rangle[1\,2][4\,6]-2\langle 2\,4\rangle\langle 4\,5\rangle[1\,4][4\,6]-3\langle 2\,5\rangle\langle 4\,5\rangle[1\,4][5\,6]\Big]/(4\langle 3\,4\rangle^2 s_{12}s_{56})\,, \qquad \text{(C.43)}$$

$$c^{(2)}_{4|123}(3^-_g,4^-_g)=\Big[$$
$$\times 2\frac{\langle 4\,5\rangle}{s_{123}}\Big(2\langle 1\,2\rangle\langle 1\,3\rangle[1\,3][1\,4][1\,6]+\langle 1\,2\rangle\langle 2\,3\rangle[1\,3][1\,6][2\,4]-2\langle 1\,2\rangle\langle 2\,4\rangle[1\,2][1\,4][4\,6]$$
$$-2\langle 1\,2\rangle\langle 3\,4\rangle[1\,4]^2[3\,6]+2\langle 1\,3\rangle\langle 2\,3\rangle[1\,3][1\,6][3\,4]-\langle 1\,4\rangle\langle 2\,3\rangle[1\,4]^2[3\,6]$$
$$-\langle 2\,3\rangle^2[1\,2][3\,4][3\,6]+2\langle 2\,3\rangle^2[1\,3][2\,6][3\,4]-2\langle 2\,3\rangle\langle 2\,4\rangle[1\,4][2\,3][4\,6]$$
$$-\langle 2\,3\rangle\langle 2\,4\rangle[1\,6][2\,4][3\,4]+\langle 2\,3\rangle\langle 2\,5\rangle[1\,2][3\,4][5\,6]+\langle 2\,3\rangle\langle 3\,4\rangle[1\,4][3\,4][3\,6]$$
$$-2\langle 2\,3\rangle\langle 3\,4\rangle[1\,6][3\,4]^2+\langle 2\,3\rangle\langle 4\,5\rangle[1\,4][3\,4][5\,6]\Big)$$
$$+\frac{\langle 2|(5+6)|4]}{\langle 3|(5+6)|4]}\langle 4\,5\rangle\Big(2\langle 2\,3\rangle[1\,2][4\,6]-\langle 1\,3\rangle[1\,4][1\,6]-\langle 2\,3\rangle[1\,4][2\,6]-4\langle 3\,4\rangle[1\,4][4\,6]\Big)$$
$$-2\frac{\langle 4|(5+6)|1]\langle 1\,2\rangle\langle 2\,3\rangle\langle 4\,5\rangle[1\,4][2\,6][3\,4]}{\langle 4|(5+6)|4]s_{123}}+\frac{\langle 4|(5+6)|3]}{s_{123}}\Big(2\langle 1\,5\rangle\langle 2\,3\rangle[1\,4][1\,6]\Big)$$
$$+2\frac{\langle 4|(5+6)|3]}{\langle 4|(5+6)|4]s_{123}}[1\,4][1\,6]\Big(\langle 1\,3\rangle\langle 2\,3\rangle\langle 4\,5\rangle[3\,4]+\langle 1\,4\rangle\langle 2\,3\rangle\langle 5\,6\rangle[4\,6]-2\langle 1\,2\rangle\langle 1\,3\rangle\langle 4\,5\rangle[1\,4]\Big)$$
$$+2\frac{\langle 4|(5+6)|4]}{\langle 4|(5+6)|3]}\langle 4\,5\rangle[1\,3]\Big(2\langle 2\,4\rangle[4\,6]+\langle 2\,5\rangle[5\,6]\Big)$$
$$+4\frac{\langle 5|(2+3)|1]}{\langle 4|(5+6)|4]s_{123}}\Big(\langle 2\,3\rangle\langle 3\,4\rangle\langle 4\,5\rangle[3\,4]^2[5\,6]\Big)$$
$$-8\frac{\langle 1\,2\rangle\langle 2\,4\rangle\langle 4\,5\rangle[1\,2][1\,4][1\,6][3\,4]}{[1\,3]\langle 4|(5+6)|4]}+\frac{1}{\langle 3|(5+6)|4]}s_{123}[1\,4][4\,6]\Big(\langle 2\,3\rangle\langle 4\,5\rangle+4\langle 2\,5\rangle\langle 3\,4\rangle\Big)$$
$$+\frac{\langle 2\,4\rangle\langle 3\,4\rangle\langle 5\,6\rangle[1\,4][4\,6]^2}{\langle 3|(5+6)|4]\langle 4|(5+6)|4]}s_{123}-\frac{\langle 2\,3\rangle\langle 5\,6\rangle[4\,6]}{\langle 3|(5+6)|4]}\Big(\langle 2\,4\rangle[1\,2][4\,6]+4\langle 3\,4\rangle[1\,4][3\,6]\Big)$$
$$+\frac{\langle 2\,4\rangle\langle 4\,5\rangle[1\,4][3\,6]s_{123}}{\langle 4|(5+6)|3]}-\frac{\langle 2\,4\rangle\langle 4\,5\rangle^2[1\,4][3\,4][5\,6]s_{123}}{\langle 4|(5+6)|3]\langle 4|(5+6)|4]}-4\frac{\langle 2\,4\rangle\langle 4\,5\rangle[1\,4][4\,6]s_{123}}{\langle 4|(5+6)|4]}$$
$$+2\frac{\langle 4\,5\rangle[3\,4][5\,6]}{\langle 4|(5+6)|3]}\Big(2\langle 2\,3\rangle\langle 4\,5\rangle[1\,3]+\langle 2\,4\rangle\langle 2\,5\rangle[1\,2]+\langle 2\,5\rangle\langle 3\,4\rangle[1\,3]\Big)$$
$$+2\frac{\langle 4\,5\rangle[1\,4][5\,6]}{\langle 4|(5+6)|4]s_{123}}\Big(2\langle 1\,2\rangle\langle 3\,4\rangle\langle 4\,5\rangle[1\,4][3\,4]-\langle 1\,2\rangle\langle 2\,3\rangle\langle 4\,5\rangle[1\,2][3\,4]$$
$$-\langle 1\,4\rangle\langle 2\,3\rangle\langle 5\,6\rangle[1\,3][4\,6]\Big)$$
$$+2\frac{\langle 4\,5\rangle}{\langle 4|(5+6)|4]}\Big(2\langle 2\,3\rangle\langle 2\,4\rangle[1\,2][3\,4][4\,6]-2\langle 2\,5\rangle\langle 3\,4\rangle[1\,4][3\,4][5\,6]$$
$$-\langle 1\,2\rangle\langle 4\,5\rangle[1\,4]^2[5\,6]-\langle 1\,4\rangle\langle 2\,3\rangle[1\,3][1\,4][4\,6]-\langle 2\,3\rangle\langle 4\,5\rangle[1\,4][3\,4][5\,6]\Big)$$
$$+\langle 2\,3\rangle\langle 4\,5\rangle[1\,3][4\,6]+4\langle 2\,3\rangle\langle 4\,5\rangle[1\,6][3\,4]-\langle 2\,4\rangle\langle 2\,5\rangle[1\,2][4\,6]-5\langle 2\,4\rangle\langle 4\,5\rangle[1\,4][4\,6]$$
$$-\langle 2\,5\rangle\langle 3\,4\rangle[1\,3][4\,6]+\langle 2\,5\rangle\langle 4\,5\rangle[1\,4][5\,6]\Big]/(4[3\,4]^2 s_{12}s_{56})\,, \qquad \text{(C.44)}$$

JHEP01(2017)020

$$
\begin{aligned}
c^{(2)}_{4|123}(3_g^+,4_g^-) = \Bigg[& \\
&\times 2\frac{\langle 4\,5\rangle}{s_{123}}\Big(3\langle 1\,4\rangle\langle 2\,4\rangle[1\,3][1\,6][3\,4] - \langle 1\,2\rangle\langle 2\,4\rangle[1\,3]^2[2\,6] - 2\langle 1\,4\rangle\langle 2\,5\rangle[1\,3]^2[5\,6] \\
&\quad -4\langle 2\,4\rangle^2[1\,2][3\,4][3\,6] + 2\langle 2\,4\rangle^2[1\,3][2\,6][3\,4] - \langle 2\,4\rangle\langle 2\,5\rangle[1\,3][2\,3][5\,6] + \langle 2\,4\rangle\langle 3\,4\rangle[1\,3][3\,4][3\,6]\Big) \\
&-\frac{\langle 2|(5+6)|4]\langle 4|(5+6)|3]\langle 2\,5\rangle\langle 3\,4\rangle[1\,2][4\,6]}{\langle 3|(5+6)|4]^2} + \frac{\langle 2|(5+6)|4]\langle 4|(5+6)|3]\langle 4\,5\rangle[1\,6]}{\langle 3|(5+6)|4]} \\
&+\frac{\langle 2|(5+6)|4]}{\langle 3|(5+6)|4]}\langle 4\,5\rangle[3\,6]\Big(\langle 3\,4\rangle[1\,3] - \langle 2\,4\rangle[1\,2]\Big) - \frac{\langle 4|(5+6)|1]\langle 4|(5+6)|3]\langle 2\,5\rangle[4\,6]}{\langle 3|(5+6)|4]} \\
&+4\frac{\langle 4|(5+6)|1]}{\langle 1\,3\rangle\langle 4|(5+6)|4]s_{123}}\Big(\langle 1\,2\rangle\langle 1\,4\rangle\langle 2\,5\rangle\langle 4\,5\rangle[1\,2][3\,4][5\,6]\Big) \\
&-\frac{\langle 4|(5+6)|1]}{\langle 3|(5+6)|4]^2}s_{123}\Big(\langle 2\,4\rangle\langle 3\,5\rangle[3\,4][4\,6]\Big) + \frac{\langle 4|(5+6)|1]}{\langle 3|(5+6)|4]}\langle 4\,5\rangle[3\,4]\Big(3\langle 2\,4\rangle[4\,6] + \langle 2\,5\rangle[5\,6]\Big) \\
&-4\frac{\langle 4|(5+6)|3]\langle 4|(5+6)|4]}{\langle 3|(5+6)|4]^2}\Big(\langle 2\,5\rangle\langle 3\,4\rangle[1\,4][4\,6]\Big) - \frac{\langle 4|(5+6)|3]}{\langle 3|(5+6)|4]}\Big(\langle 2\,3\rangle\langle 4\,5\rangle[1\,3][4\,6]\Big) \\
&+4\frac{\langle 4|(5+6)|3]}{\langle 1\,3\rangle\langle 4|(5+6)|4]s_{123}}\langle 1\,2\rangle\langle 3\,4\rangle\langle 4\,5\rangle[1\,2][3\,4]\Big(\langle 1\,2\rangle[1\,6] - \langle 2\,3\rangle[3\,6]\Big) \\
&+3\frac{\langle 4|(5+6)|3]}{\langle 3|(5+6)|4]^2}s_{123}\Big(\langle 2\,5\rangle\langle 3\,4\rangle[1\,4][4\,6]\Big) - \frac{\langle 4|(5+6)|3]}{\langle 3|(5+6)|4]^2}\langle 2\,4\rangle\langle 5\,6\rangle[4\,6]^2\Big(\langle 2\,3\rangle[1\,2] + 4\langle 3\,4\rangle[1\,4]\Big) \\
&+2\frac{\langle 4|(5+6)|3]\langle 4\,5\rangle}{\langle 4|(5+6)|4]s_{123}}\Big(\langle 1\,2\rangle\langle 2\,4\rangle[1\,3][1\,4][2\,6] + 2\langle 1\,2\rangle\langle 3\,4\rangle[1\,3][1\,6][3\,4] \\
&\quad +2\langle 1\,4\rangle\langle 2\,5\rangle[1\,3][1\,4][5\,6] - \langle 2\,3\rangle\langle 2\,4\rangle[1\,3][2\,6][3\,4] - 2\langle 2\,3\rangle\langle 3\,4\rangle[1\,3][3\,4][3\,6] \\
&\quad -2\langle 2\,4\rangle\langle 2\,5\rangle[1\,2][3\,4][5\,6] + \langle 2\,4\rangle\langle 2\,5\rangle[1\,3][2\,4][5\,6]\Big) \\
&+\frac{\langle 4|(5+6)|4]}{\langle 3|(5+6)|4]}\langle 4\,5\rangle[1\,6]\Big(\langle 2\,4\rangle[3\,4] - \langle 1\,2\rangle[1\,3]\Big) \\
&+4\frac{\langle 1\,2\rangle\langle 2\,4\rangle\langle 4\,5\rangle[1\,2][3\,4]}{\langle 1\,3\rangle s_{123}}\Big(2\langle 1\,4\rangle[1\,6] + \langle 3\,4\rangle[3\,6]\Big) \\
&+4\frac{\langle 1\,2\rangle\langle 2\,4\rangle\langle 4\,5\rangle[1\,2][3\,4][5\,6]}{\langle 1\,3\rangle\langle 4|(5+6)|4]s_{123}}\Big(\langle 2\,5\rangle\langle 3\,4\rangle[2\,3] - \langle 3\,4\rangle\langle 4\,5\rangle[3\,4] - \langle 1\,4\rangle\langle 2\,5\rangle[1\,2] - 2\langle 1\,4\rangle\langle 4\,5\rangle[1\,4]\Big) \\
&\quad +\frac{\langle 2\,4\rangle\langle 3\,4\rangle\langle 5\,6\rangle[1\,3][4\,6]^2 s_{123}}{\langle 3|(5+6)|4]^2} + \frac{\langle 2\,4\rangle}{\langle 3|(5+6)|4]}\Big(2\langle 2\,4\rangle\langle 5\,6\rangle[1\,2][3\,6][4\,6] \\
&\quad -\langle 2\,5\rangle\langle 4\,5\rangle[1\,2][3\,4][5\,6] - \langle 3\,4\rangle\langle 5\,6\rangle[1\,3][3\,6][4\,6] - \langle 4\,5\rangle^2[1\,4][3\,4][5\,6]\Big) \\
&+2\frac{\langle 2\,4\rangle\langle 4\,5\rangle[3\,4][5\,6]}{\langle 4|(5+6)|4]s_{123}}\Big(4\langle 2\,4\rangle\langle 4\,5\rangle[1\,2][3\,4] - 3\langle 1\,4\rangle\langle 4\,5\rangle[1\,3][1\,4] - 2\langle 1\,4\rangle\langle 2\,5\rangle[1\,2][1\,3] \\
&\quad -2\langle 2\,4\rangle\langle 2\,5\rangle[1\,2][2\,3] - 2\langle 2\,4\rangle\langle 4\,5\rangle[1\,3][2\,4] - \langle 1\,3\rangle\langle 4\,5\rangle[1\,3]^2 - \langle 3\,4\rangle\langle 4\,5\rangle[1\,3][3\,4]\Big) \\
&-2\frac{\langle 2\,4\rangle\langle 4\,5\rangle^2[1\,3][3\,4][5\,6]}{\langle 4|(5+6)|4]} + \langle 2\,4\rangle\langle 4\,5\rangle[1\,3][3\,6]\Bigg]/(4\langle 3\,4\rangle[3\,4]s_{12}s_{56})\,,
\end{aligned}
\tag{C.45}
$$

$$
\begin{aligned}
c^{(2)}_{4|123}(3_g^-,4_g^+) = \Bigg[& \\
&\times 2\frac{\langle 2\,3\rangle\langle 3\,4\rangle[1\,4][4\,6]}{s_{123}}\Big(\langle 1\,5\rangle[1\,4] - \langle 3\,5\rangle[3\,4]\Big) - 4\frac{\langle 2|(5+6)|4]}{\langle 4|(5+6)|4]s_{123}}\Big(\langle 2\,3\rangle\langle 3\,4\rangle\langle 5\,6\rangle[1\,2][4\,6]^2\Big) \\
&+4\frac{\langle 3|(5+6)|4]}{\langle 4|(5+6)|3]^2}\langle 2\,4\rangle\langle 4\,5\rangle[3\,4][5\,6]\Big(\langle 2\,5\rangle[1\,2] + \langle 3\,5\rangle[1\,3]\Big)
\end{aligned}
$$

JHEP01(2017)020

$$
\begin{aligned}
&+\frac{\langle 3|(5+6)|4]}{\langle 4|(5+6)|3]}\Big(4\langle 2\,3\rangle\langle 4\,5\rangle[1\,3][4\,6]+2\langle 2\,4\rangle\langle 2\,5\rangle[1\,2][4\,6]+\langle 2\,4\rangle\langle 4\,5\rangle[1\,4][4\,6]\\
&\quad+2\langle 2\,5\rangle\langle 3\,4\rangle[1\,3][4\,6]+3\langle 2\,5\rangle\langle 4\,5\rangle[1\,4][5\,6]\Big)\\
&+4\frac{\langle 3|(5+6)|4]\langle 3\,4\rangle[4\,6]}{\langle 4|(5+6)|4]s_{123}}\Big(\langle 1\,2\rangle\langle 2\,5\rangle[1\,2][1\,4]+\langle 2\,3\rangle\langle 2\,5\rangle[1\,2][3\,4]+\langle 2\,3\rangle\langle 3\,5\rangle[1\,3][3\,4]\Big)\\
&-4\frac{\langle 3|(5+6)|4]}{\langle 4|(5+6)|4]}\Big(\langle 2\,5\rangle\langle 3\,4\rangle[1\,4][4\,6]\Big)-8\frac{\langle 1\,2\rangle\langle 2\,5\rangle\langle 3\,4\rangle[1\,2][1\,4]^2[4\,6]}{[1\,3]\langle 4|(5+6)|4]}\\
&-\frac{\langle 4|(5+6)|4]}{\langle 4|(5+6)|3]}\langle 2\,5\rangle\Big(2\langle 2\,3\rangle[1\,2][4\,6]+2\langle 3\,4\rangle[1\,4][4\,6]+\langle 3\,5\rangle[1\,4][5\,6]\Big)\\
&+\frac{[1\,4]}{\langle 4|(5+6)|3]}\Big(\langle 1\,2\rangle\langle 2\,4\rangle\langle 3\,5\rangle[1\,2][4\,6]+\langle 1\,2\rangle\langle 3\,4\rangle\langle 3\,5\rangle[1\,3][4\,6]-\langle 2\,4\rangle\langle 3\,4\rangle\langle 5\,6\rangle[4\,6]^2\\
&\quad-2\langle 1\,2\rangle\langle 3\,5\rangle\langle 4\,5\rangle[1\,4][5\,6]-2\langle 2\,3\rangle\langle 3\,5\rangle\langle 4\,5\rangle[3\,4][5\,6]+\langle 2\,3\rangle\langle 4\,5\rangle\langle 5\,6\rangle[4\,6][5\,6]\Big)\\
&+2\frac{\langle 3\,4\rangle[1\,4][4\,6]}{\langle 4|(5+6)|4]s_{123}}\Big(2\langle 1\,2\rangle\langle 2\,3\rangle\langle 3\,5\rangle[1\,2][3\,4]-2\langle 1\,2\rangle^2\langle 3\,5\rangle[1\,2][1\,4]\\
&\quad+5\langle 1\,2\rangle\langle 2\,3\rangle\langle 5\,6\rangle[1\,2][4\,6]+\langle 1\,2\rangle\langle 2\,3\rangle\langle 5\,6\rangle[1\,4][2\,6]+2\langle 1\,3\rangle\langle 2\,3\rangle\langle 5\,6\rangle[1\,4][3\,6]\\
&\quad+\langle 1\,4\rangle\langle 2\,3\rangle\langle 5\,6\rangle[1\,4][4\,6]+\langle 2\,3\rangle^2\langle 5\,6\rangle[2\,4][3\,6]-\langle 2\,3\rangle\langle 3\,4\rangle\langle 5\,6\rangle[3\,4][4\,6]\Big)\\
&+2\frac{\langle 3\,4\rangle[1\,4][4\,6]}{\langle 4|(5+6)|4]}\Big(\langle 2\,3\rangle\langle 3\,5\rangle[3\,4]-\langle 1\,2\rangle\langle 3\,5\rangle[1\,4]-\langle 1\,3\rangle\langle 2\,5\rangle[1\,4]-\langle 2\,3\rangle\langle 5\,6\rangle[4\,6]\Big)\\
&-3\langle 2\,3\rangle\langle 3\,5\rangle[1\,4][4\,6]\Big]/(4\langle 3\,4\rangle[3\,4]s_{12}s_{56})\,.
\end{aligned}
\tag{C.46}
$$

C.6.3 BDK contribution

The final contribution in eq. (C.24) that must be specified is $A^{\rm ax}_{6,BDK}$. This consists of terms representing the contributions of the bubble integrals and rational terms, as well as the mass-independent coefficient of the triangle $c_{12|34}$. Although the bubble and triangle coefficients are the same as in the original BDK paper, the integrals that they multiply are of course the ones with non-zero masses in the loop. Our recasting therefore necessitates the introduction of the following functions related to scalar bubble integrals,

$$
\begin{aligned}
\overline{L}_{-1}(x,y,m^2) &= B_0^{p_y}-B_0^{p_x}\\
\overline{L}_0(x,y,m^2) &= \frac{y}{(y-x)}\,\overline{L}_{-1}(x,y,m^2)\\
\overline{L}_1(x,y,m^2) &= \frac{y}{(y-x)}\left[\overline{L}_0(x,y,m^2)+1\right]
\end{aligned}
\tag{C.47}
$$

such that $x=p_x^2, y=p_y^2$. In the limit $m\to 0$ these reduce to the standard BDK functions,

$$
\overline{L}_i(x,y,m^2)\big|_{m\to 0} = L_i\left(\frac{-p_x^2}{-p_y^2}\right)\,,
\tag{C.48}
$$

with $L_{-1}(x,y,0)\equiv \ln(-x)-\ln(-y)$. The overall sign of our expressions is also opposite to the one of BDK, due to the fact that our result describes the amplitudes for a top quark ($\tau_3^f=+1/2$) rather than the (massless) bottom quark ($\tau_3^f=-1/2$) in BDK. As in the

JHEP01(2017)020

massless case, we only need consider three helicity combinations. The final one is related by,

$$A^{\rm ax}_{6,BDK}(1_q^+,2_{\bar q}^-,3_g^-,4_g^-,5_{\bar e}^-,6_e^+) = {\rm flip}_2\left[A^{\rm ax}_{6,BDK}(1_q^+,2_{\bar q}^-,3_g^+,4_g^+,5_{\bar e}^-,6_e^+)\right]\,. \tag{C.49}$$

With the preliminaries understood we can make use of BDK eq. (11.3) to write the amplitude with two gluons of positive helicity as,

$$\begin{aligned}
-iA^{\rm ax}_{6,BDK}(1_q^+,2_{\bar q}^-,3_g^+,4_g^+,5_{\bar e}^-,6_e^+) = \Bigg[&-\frac{\langle 2\,5\rangle^2}{\langle 1\,2\rangle\langle 5\,6\rangle\langle 3\,4\rangle^2}\overline{L}_{-1}(s_{123},s_{56},m_t^2)\\
&+\frac{\langle 2|4|6]\langle 2\,5\rangle}{\langle 1\,2\rangle\langle 3\,4\rangle^2 s_{56}}\left(\frac{s_{34}}{s_{56}}\overline{L}_1(s_{123},s_{56},m_t^2)+\overline{L}_0(s_{123},s_{56},m_t^2)\right)\\
&+\frac{\langle 5|3|1]\langle 2\,5\rangle}{\langle 5\,6\rangle\langle 3\,4\rangle^2}\frac{\overline{L}_0(s_{123},s_{12},m_t^2)}{s_{12}} - {\rm exch}_{34}\Bigg]\\
&-(s_{14}+s_{34})\frac{\langle 2\,5\rangle[4\,6]}{\langle 1\,3\rangle\langle 3\,4\rangle}\frac{1}{s_{56}^2}\overline{L}_1(s_{123},s_{56},m_t^2)\\
&-\frac{\langle 2|3|1]\langle 2\,5\rangle[3\,6]}{\langle 2\,4\rangle\langle 3\,4\rangle}\frac{1}{s_{56}^2}\overline{L}_1(s_{124},s_{56},m_t^2)\,.
\end{aligned} \tag{C.50}$$

The amplitudes with gluons of opposite helicity are not related by a symmetry, but do share a common structure. We note also that the recasting of BDK eqs. (11.9) and (11.10) also requires the following replacements to be made in the BDK formulae,

$$\begin{aligned}
Ls_{-1}^{2mh}(s_{34},s_{123},s_{12},s_{56}) &\longrightarrow \left(\frac{\delta_{34}}{2}+\frac{s_{12}s_{56}}{s_{123}}\right) I_3^{3m}(s_{12},s_{34},s_{56})\,,\\
I_3^{3m}(s_{12},s_{34},s_{56}) &\longrightarrow -C_0^{12|34}\,.
\end{aligned} \tag{C.51}$$

in order to isolate the contribution of the triangle with three off-shell legs (cf. BDK eq. (B.3)) in the notation of this paper. By adapting the formulae in this way we obtain,

$$\begin{aligned}
-iA^{\rm ax}_{6,BDK}(1_q^+,2_{\bar q}^-,3_g^+,4_g^-,5_{\bar e}^-,6_e^+) = &-C^{\rm ax}+\frac{\langle 2\,4\rangle\langle 1\,4\rangle[4\,6]\langle 2|(1+3)|6]}{\langle 1\,2\rangle\langle 1\,3\rangle[5\,6]\langle 3|(1+2)|4]}\frac{\overline{L}_1(s_{56},s_{123},m_t^2)}{s_{123}}\\
&+\frac{\langle 2|(1+3)|6]\langle 3|(1+2)|6][1\,3]}{[5\,6]\langle 3|(1+2)|4]^2}\frac{\overline{L}_0(s_{123},s_{12},m_t^2)}{s_{12}}\\
&+\frac{\langle 2\,4\rangle\langle 1|(2+3)|4]\langle 2|(1+3)|6]\langle 3|(1+2)|6]}{\langle 1\,2\rangle\langle 1\,3\rangle[5\,6]\langle 3|(1+2)|4]^2}\frac{\overline{L}_0(s_{123},s_{56},m_t^2)}{s_{56}}\\
&-\frac{\langle 2\,4\rangle\langle 3\,5\rangle\langle 4|(1+3)|6]}{\langle 1\,3\rangle\langle 3\,4\rangle s_{56}\langle 3|(1+2)|4]}+{\rm flip}_2\,,
\end{aligned} \tag{C.52}$$

and,

$$\begin{aligned}
-iA^{\rm ax}_{6,BDK}(1_q^+,2_{\bar q}^-,3_g^-,4_g^+,5_{\bar e}^-,6_e^+) = &\,C^{\rm ax}(3\leftrightarrow 4)\\
&-\frac{[1\,4]^2\langle 4\,5\rangle\langle 5|(2+3)|1]}{[1\,2][1\,3]\langle 5\,6\rangle\langle 4|(1+2)|3]}\frac{\overline{L}_1(s_{56},s_{123},m_t^2)}{s_{123}}\\
&+\frac{\langle 5|(2+3)|1]\langle 5|(1+2)|3]\langle 2\,3\rangle}{\langle 5\,6\rangle\langle 4|(1+2)|3]^2}\frac{\overline{L}_0(s_{123},s_{12},m_t^2)}{s_{12}}
\end{aligned}$$

$$
\begin{aligned}
&-\frac{[1\,4]\langle 4|(2+3)|1]\langle 5|(2+3)|1]\langle 5|(1+2)|3]}{[1\,2][1\,3]\langle 5\,6\rangle\langle 4|(1+2)|3]^2}\frac{\overline{L}_0(s_{123},s_{56},m_t^2)}{s_{56}}\\
&\quad-\frac{[1\,4]^2\langle 2\,5\rangle[3\,6]}{[1\,3][3\,4]s_{56}\langle 4|(1+2)|3]}+\text{flip}_2\,. \qquad \text{(C.53)}
\end{aligned}
$$

The auxiliary common quantity is adapted from BDK eq. (11.9) and is given by,

$$
\begin{aligned}
C^{\text{ax}} = -\Bigg[&-\frac{3}{2}\left(\langle 5|2|1]\langle 2|1|6]+\langle 5|6|1]\langle 2|5|6]-\langle 5|3|1]\langle 2|4|6]-\langle 5|4|1]\langle 2|3|6]\right)\frac{\langle 4|(1+2)|3]}{\langle 3|(1+2)|4]\Delta_3}\\
&-3\frac{\delta_{34}(\langle 5|2|1]\delta_{12}-\langle 5|6|1]\delta_{56})\langle 4|(1+2)|3]\langle 2|(1+3)|6]}{\langle 3|(1+2)|4]\Delta_3^2}-\frac{[1\,3]\langle 4\,5\rangle\langle 2\,4\rangle[3\,6]}{\Delta_3}\\
&+\frac{[1\,4]\langle 3\,5\rangle(s_{123}-s_{124})\langle 4|(1+2)|3]\langle 2|(1+3)|6]}{\langle 3|(1+2)|4]^2\Delta_3}-\frac{1}{2}\frac{[1\,3]\langle 4\,5\rangle\langle 2|(1+3)|6]}{s_{123}\langle 3|(1+2)|4]}\\
&-\frac{1}{2}\frac{\langle 2|(1+3)|4]^2\langle 3|(1+2)|6]^2-\langle 2\,3\rangle^2[4\,6]^2s_{123}^2}{\langle 1\,2\rangle[5\,6]\langle 3|(1+2)|4]^4}\left(\frac{\delta_{34}}{2}+\frac{s_{12}s_{56}}{s_{123}}\right)\Bigg]C_0^{12|34}\\
&+C_1^{\text{ax}}+C_1^{\text{ax}}(1\leftrightarrow 6,2\leftrightarrow 5)\\
&+\frac{\langle 2|(1+3)|6]^2}{\langle 1\,2\rangle[5\,6]\langle 3|(1+2)|4]^2}\overline{L}_{-1}(s_{56},s_{34},m_t^2) \qquad \text{(C.54)}\\
&+\frac{\langle 2\,4\rangle[3\,6]}{\langle 3|(1+2)|4]}\left(\frac{\langle 2|4|6]\delta_{34}}{\langle 1\,2\rangle[5\,6]\Delta_3}-\frac{\langle 2\,4\rangle\langle 3\,5\rangle\delta_{56}}{\langle 1\,2\rangle\langle 3\,4\rangle\Delta_3}-\frac{[1\,3][4\,6]\delta_{12}}{[3\,4][5\,6]\Delta_3}-2\frac{\langle 5|3|1]}{\Delta_3}+\frac{\langle 2\,4\rangle\langle 3\,5\rangle}{\langle 1\,2\rangle\langle 3\,4\rangle s_{56}}\right),
\end{aligned}
$$

where the function C_1^{ax} is defined as,

$$
\begin{aligned}
C_1^{\text{ax}} = \Bigg(&-6\frac{[1\,2]\langle 2|(1+3)|6](\langle 2\,5\rangle\delta_{34}-2\langle 2\,1\rangle[1\,6]\langle 6\,5\rangle)\langle 4|(1+2)|3]}{\langle 3|(1+2)|4]\Delta_3^2}-\frac{[1\,3][4\,6]\langle 2|(1+3)|6]}{[3\,4][5\,6]\langle 3|(1+2)|4]^2}\\
&+[1\,4]\frac{\langle 2|(1+3)|6](3\langle 3|(1+2)|4][3\,6]-[4\,6](s_{123}-s_{124}))\langle 4|(1+2)|3]}{[3\,4][5\,6]\langle 3|(1+2)|4]^2\Delta_3}\\
&-\frac{[1\,3]\langle 2\,4\rangle[3\,6]^2}{[3\,4][5\,6]\Delta_3}\Bigg)\overline{L}_{-1}(s_{12},s_{34},m_t^2)\,. \qquad \text{(C.55)}
\end{aligned}
$$

These functions are defined in terms of the additional quantities,

$$
\begin{aligned}
\Delta_3 &= s_{12}^2+s_{34}^2+s_{56}^2-2s_{12}s_{34}-2s_{34}s_{56}-2s_{56}s_{12}\,,\\
\delta_{12} &= s_{12}-s_{34}-s_{56},\ \delta_{34}=s_{34}-s_{56}-s_{12},\ \delta_{56}=s_{56}-s_{12}-s_{34}\,. \qquad \text{(C.56)}
\end{aligned}
$$

Finally, we note that the determination of the triangle coefficient $c_{12|34}^{(2)}$ using eq. (C.28) requires knowledge of the rational part of the amplitudes. We do not list these explicitly here since they may be simply obtained from the expressions for $A_{6,BDK}^{\text{ax}}$ through the relation,

$$
R(3^{h_3},4^{h_4}) = \left[A_{6,BDK}^{\text{ax}}(1_q^+,2_{\bar{q}}^-,3_g^{h_3},4_g^{h_4},5_{\bar{e}}^-,6_e^+)\right]_{C_0^{12|34}\to 0,\ \overline{L}_{-1}(x,y,m^2)\to 0} \qquad \text{(C.57)}
$$

JHEP01(2017)020

D Definition of scalar integrals

The scalar integrals themselves are defined as follows,

$$\begin{aligned} B_0^x &\equiv B_0(p_x; m_1, m_2) = \frac{\mu^{4-d}}{i\pi^{\frac{d}{2}} r_\Gamma} \int d^d l \, \frac{1}{d(l, m_1)\, d(l + p_x, m_2)} \\ C_0^{x|y} &\equiv C_0(p_x, p_y; m_1, m_2, m_3) = \frac{1}{i\pi^2} \\ &\quad \times \int d^4 l \, \frac{1}{d(l, m_1)\, d(l + p_x, m_2)\, d(l + p_x + p_y, m_3)} \qquad \text{(D.1)} \\ D_0^{x|y|z} &\equiv D_0(p_x, p_y, p_z; m_1, m_2, m_3, m_4) = \frac{1}{i\pi^2} \\ &\quad \times \int d^4 l \, \frac{1}{d(l, m_1)\, d(l + p_x, m_2)\, d(l + p_x + p_y, m_3)\, d(l + p_x + p_y + p_z, m_4)} \qquad \text{(D.2)} \end{aligned}$$

where the denominator function is

$$d(l, m) = (l^2 - m^2 + i\varepsilon)\,. \qquad \text{(D.3)}$$

For the purposes of this paper we take the masses in the propagators to be real. Near four dimensions we use $d = 4 - 2\epsilon$ (and for clarity the small imaginary part which fixes the analytic continuations is specified by $+i\,\varepsilon$). μ is a scale introduced so that the integrals preserve their natural dimensions, despite excursions away from $d = 4$. We have removed the overall constant which occurs in d-dimensional integrals

$$r_\Gamma \equiv \frac{\Gamma^2(1-\epsilon)\Gamma(1+\epsilon)}{\Gamma(1-2\epsilon)} = \frac{1}{\Gamma(1-\epsilon)} + \mathcal{O}(\epsilon^3) = 1 - \epsilon\gamma + \epsilon^2\left[\frac{\gamma^2}{2} - \frac{\pi^2}{12}\right] + \mathcal{O}(\epsilon^3)\,. \qquad \text{(D.4)}$$

E Numerical values of coefficients

The test momenta are, in the notation $p = (E, p_x, p_y, p_z)$ (in GeV),

$$\begin{aligned} p_1 &= (-3.0, 2.1213203435596424, 1.0606601717798212, 1.8371173070873839)\,, \\ p_2 &= (-3.0, -2.1213203435596424, -1.0606601717798212, -1.8371173070873839)\,, \\ p_3 &= (0.85714285714285710, -0.31578947368421051, 0.79685060448070799, 0.0)\,, \\ p_4 &= (2.0, 2.0, 0.0, 0.0)\,, \qquad \text{(E.1)} \\ p_5 &= (1.0, -0.18421052631578949, 0.46482951928041311, 0.86602540378443860)\,, \\ p_6 &= (2.1428571428571432, -1.5, -1.2616801237611210, -0.86602540378443860)\,. \end{aligned}$$

with

$$p_1 + p_2 + p_3 + p_4 + p_5 + p_6 = 0\,. \qquad \text{(E.2)}$$

We use $m_t = 0.4255266775\,\text{GeV}$.

The results for the various contributions to the A_6^{ax} partial amplitudes are shown in tables 3–7. We show results for the non-zero box and triangle coefficients as well as the remaining contribution $A_{6,BDK}^{\text{ax}}$ that includes both bubbles and rational terms. The coefficient $c_{12|34}^{(0)}$ is not shown explicitly for the amplitudes with opposite gluon helicity even though it is non-zero, since its effect is also included in $A_{6,BDK}^{\text{ax}}$.

JHEP01(2017)020

Coeff	Re $y^{(0)}(3^+,4^+)$	Im $y^{(0)}(3^+,4^+)$	Re $y^{(2)}(3^+,4^+)$	Im $y^{(2)}(3^+,4^+)$
$c_{3\|124}$			-0.13353418	-0.49827218
$c_{4\|123}$			-0.79126348	0.38570625
b_{56}	0.20772009	0.22131702		
b_{123}	-0.13126100	0.06398398		
b_{124}	-0.07645909	-0.28530101		
R	-0.46239883	-0.05628296		
Coeff	Re $y^{(0)}(3^-,4^+)$	Im $y^{(0)}(3^-,4^+)$	Re $y^{(2)}(3^-,4^+)$	Im $y^{(2)}(3^-,4^+)$
$c_{3\|124}$			0.20571266	-0.0325607
$c_{4\|123}$			-0.29104980	1.0411831
b_{56}	-0.06950546	-0.15407601		
b_{123}	-0.04828163	0.17271964		
b_{124}	0.11778709	-0.01864363		
R	-0.04266857	0.50431124		
Coeff	Re $y^{(0)}(3^+,4^-)$	Im $y^{(0)}(3^+,4^-)$	Re $y^{(2)}(3^+,4^-)$	Im $y^{(2)}(3^+,4^-)$
$c_{3\|124}$			0.01389374	-0.00477234
$c_{4\|123}$			-0.01145015	0.07951003
b_{56}	-0.00605585	-0.01045720		
b_{123}	-0.00189944	0.01318975		
b_{124}	0.00795529	-0.00273255		
R	0.00122180	0.03736885		
Coeff	Re $y^{(0)}(3^-,4^-)$	Im $y^{(0)}(3^-,4^-)$	Re $y^{(2)}(3^-,4^-)$	Im $y^{(2)}(3^-,4^-)$
$c_{3\|124}$			0.01389374	-0.00477234
$c_{4\|123}$			-0.01145015	0.07951003
b_{56}	0.03831823	-0.00009208		
b_{123}	-0.01341259	0.00497689		
b_{124}	-0.02490565	-0.00488480		
R	-0.06217526	0.01073516		

Table 3. Non-zero integral coefficients for the axial contribution to $A_6^{\mathrm{ax,sl}}(1_q^+, 2_{\bar{q}}^-, 3_g, 4_g)$. Only the contribution of the isospin $+\frac{1}{2}$ quark is included.

JHEP01(2017)020

Coeff	Re $y^{(0)}(3^+,4^+)$	Im $y^{(0)}(3^+,4^+)$	Re $y^{(2)}(3^+,4^+)$	Im $y^{(2)}(3^+,4^+)$
$d_{3\|12\|4}$	0.9847638139	-0.8139317869	-0.0826002899	0.2135941623
$d_{4\|3\|12}$			0.0291379239	-0.5509736787
$d_{3\|4\|12}$			0.2392276202	0.0407498609
$c_{12\|34}$			0.1143994146	-0.2174992557
$c_{12\|3}$	0.1299341143	-0.1073937774		
$c_{12\|4}$	0.3031796001	-0.2505854807		
$c_{3\|124}$	-0.0706659218	0.0584071421	0.0542191910	0.1995748531
$c_{4\|123}$	-0.2439114076	0.2015988454	0.1822387437	-0.0369792184
$A^{\text{ax}}_{6,BDK}$	0.0744415301	-0.0504750372		

Table 4. Non-zero box and triangle coefficients and $A^{\text{ax}}_{6,BDK}$ contribution for the partial amplitude $A^{\text{ax}}_6(1^+_q,2^-_{\bar{q}},3^+_g,4^+_g)$.

Coeff	Re $y^{(0)}(3^-,4^+)$	Im $y^{(0)}(3^-,4^+)$	Re $y^{(2)}(3^-,4^+)$	Im $y^{(2)}(3^-,4^+)$
$d_{3\|12\|4}$			-0.6553781232	0.2267711354
$d_{4\|3\|12}$	3.4035534642	4.4512143946	0.7044032221	0.0506388969
$d_{3\|4\|12}$	-1.5958557084	0.0483030299	-0.5569345916	0.1188692057
$c_{12\|34}$	—	—	0.0862624911	0.0311702697
$c_{12\|3}$	0.2901747505	0.3794945606		
$c_{12\|4}$	-0.6802846449	0.0205907147		
$c_{3\|124}$	0.1585625864	-0.0047993395	-0.0253157939	0.0094553225
$c_{4\|123}$	-0.5447140053	-0.7123845260	0.0537029872	-0.2691326008
$c_{3\|4}$	0.0006275632	-0.1771280345		
$A^{\text{ax}}_{6,BDK}$	0.2424976515	0.0640430134		

Table 5. Non-zero box and triangle coefficients and $A^{\text{ax}}_{6,BDK}$ contribution for the partial amplitude $A^{\text{ax}}_6(1^+_q,2^-_{\bar{q}},3^-_g,4^+_g)$. Note that the coefficient $c^{(0)}_{12|34}$ is non-zero, but not listed explicitly here since it is included in $A^{\text{ax}}_{6,BDK}$.

F Axial triangle

The amplitude for a Z coupling to two gluons is denoted by $T^{\mu\nu\rho}_{AB}$. We calculate the triangle shown in figure 9, where all momenta are outgoing $q_1+q_2+q_3=0$ and $q_i^2\neq 0$.

The result for the two triangle diagrams shown in figure 9, (including the minus sign for a fermion loop) is,

$$T^{\mu\nu\rho}_{AB}(q_1,q_2) = i\frac{g^2 e}{16\pi^2}\delta_{AB}\; 2v^f_A\;\Gamma^{\mu\nu\rho}\,, \tag{F.1}$$

Coeff	Re $y^{(0)}(3^+,4^-)$	Im $y^{(0)}(3^+,4^-)$	Re $y^{(2)}(3^+,4^-)$	Im $y^{(2)}(3^+,4^-)$
$d_{3\|12\|4}$			0.0211964344	0.0565331937
$d_{4\|3\|12}$	-1.6787391821	3.5273786346	-0.0813082954	0.1402683777
$d_{3\|4\|12}$	-0.0292425126	-0.0031829012	-0.0630934240	-0.0104948556
$c_{12\|34}$	—	—	-0.0042375804	0.0022554921
$c_{12\|3}$	-0.1431232764	0.3007316400		
$c_{12\|4}$	-0.0124655582	-0.0013568136		
$c_{3\|124}$	0.0029055061	0.0003162498	-0.0025971585	-0.0016437585
$c_{4\|123}$	0.2686700101	-0.5645313242	-0.0144060528	-0.0236227320
$c_{3\|4}$	0.0677211776	-0.1369105940		
$A^{\rm ax}_{6,BDK}$	-0.0513599766	0.1115536722		

Table 6. Non-zero box and triangle coefficients and $A^{\rm ax}_{6,BDK}$ contribution for the partial amplitude $A^{\rm ax}_6(1^+_q,2^-_{\bar q},3^+_g,4^-_g)$. Note that the coefficient $c^{(0)}_{12|34}$ is non-zero, but not listed explicitly here since it is included in $A^{\rm ax}_{6,BDK}$.

Coeff	Re $y^{(0)}(3^-,4^-)$	Im $y^{(0)}(3^-,4^-)$	Re $y^{(2)}(3^-,4^-)$	Im $y^{(2)}(3^-,4^-)$
$d_{3\|12\|4}$	0.3650137298	1.8497925731	0.0537351845	0.2954518713
$d_{4\|3\|12}$			0.1734167739	0.0931722390
$d_{3\|4\|12}$			-0.0895807857	0.0584032726
$c_{12\|34}$			0.0357377770	0.0646139200
$c_{12\|3}$	0.0481615338	0.2440698534		
$c_{12\|4}$	0.1123769122	0.5694963246		
$c_{3\|124}$	-0.0261931149	-0.1327397448	0.0196845554	-0.0097033679
$c_{4\|123}$	-0.0904084933	-0.4581662160	-0.0075863869	-0.0498510937
$c_{3\|4}$				
$A^{\rm ax}_{6,BDK}$	0.0071292120	-0.0070092524		

Table 7. Non-zero box and triangle coefficients and $A^{\rm ax}_{6,BDK}$ contribution for the partial amplitude $A^{\rm ax}_6(1^+_q,2^-_{\bar q},3^-_g,4^-_g)$.

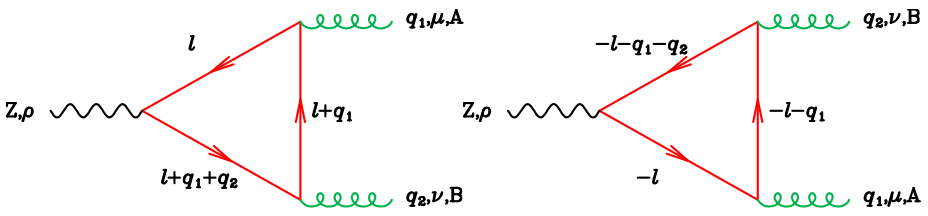

Figure 9. Triangle graphs with an axial coupling to the Z-boson.

JHEP01(2017)020

where v_A^f is given in table 1 and

$$\Gamma^{\mu\nu\rho}(q_1,q_2,m) = \frac{1}{2}\frac{1}{i\pi^2}\int d^dl\ \mathrm{Tr}\Big\{\gamma^\rho\gamma_5\frac{1}{\not l - m}\gamma^\mu\frac{1}{\not l + \not q_1 - m}\gamma^\nu\frac{1}{\not l + \not q_1 + \not q_2 - m}\Big\}. \quad \text{(F.2)}$$

The most general form of Γ consistent with QCD gauge invariance,

$$q_1^\mu\Gamma_{\mu\nu\rho} = q_2^\nu\Gamma_{\mu\nu\rho} = 0\ , \quad \text{(F.3)}$$

can be written as,

$$\begin{aligned}\Gamma^{\mu\nu\rho} = & G_1\left\{\mathrm{Tr}[\gamma^\rho\gamma^\nu\not q_1\not q_2\gamma_5]q_1^\mu + \mathrm{Tr}[\gamma^\rho\gamma^\mu\gamma^\nu\not q_2\gamma_5]q_1^2\right\}\\ & +G_2\left\{\mathrm{Tr}[\gamma^\rho\gamma^\mu\not q_2\not q_1\gamma_5]q_2^\nu + \mathrm{Tr}[\gamma^\rho\gamma^\nu\gamma^\mu\not q_1\gamma_5]q_2^2\right\}\\ & +G_3\ (q_1^\rho + q_2^\rho)\Big\{\mathrm{Tr}[\gamma^\mu\gamma^\nu\not q_1\not q_2\gamma_5]\Big\}\\ & +G_4\ (q_1^\rho - q_2^\rho)\Big\{\mathrm{Tr}[\gamma^\mu\gamma^\nu\not q_1\not q_2\gamma_5]\Big\}. \end{aligned} \quad \text{(F.4)}$$

The functions G_i are Lorentz invariant functions of $q_i^2, (i = 1, 3)$ and m. By direct calculation it is found that $G_4 = 0$. To define the other G_i we define the axial triangle function f,

$$f(m;q_1^2,q_2^2,q_3^2) = \int_0^1 d^3a_i\delta(1-a_1-a_2-a_3)\frac{a_2a_3}{[m^2 - a_1a_2q_1^2 - a_2a_3q_2^2 - a_3a_1q_3^2]}\,. \quad \text{(F.5)}$$

Full results for the function f have been given in ref. [15]. We further define the integral

$$I[j,k] = \int_0^1 d^3a_i\delta(1-a_1-a_2-a_3)\frac{a_ja_k}{[m^2 - a_1a_2q_1^2 - a_2a_3q_2^2 - a_3a_1q_3^2]}\,, \quad \text{(F.6)}$$

so that we have,

$$\begin{aligned} G_1 &= f(m;q_2^2,q_1^2,q_3^2) = I[1,2]\\ G_2 &= f(m;q_1^2,q_2^2,q_3^2) = I[2,3]\\ G_3 &= f(m;q_1^2,q_3^2,q_2^2) = I[3,1]\ . \end{aligned} \quad \text{(F.7)}$$

Contracting with the momentum of the Z boson we find that,

$$(q_3)_\rho\,\Gamma^{\mu\nu\rho} = \Big[-q_1^2\,G_1 - q_2^2\,G_2 - q_3^2\,G_3\Big]\mathrm{Tr}[\gamma^\mu\gamma^\nu\not q_1\not q_2\gamma_5]\,. \quad \text{(F.8)}$$

The divergence of the axial current is easily seen to be,

$$(q_3)_\rho\,\Gamma^{\mu\nu\rho} = \left[m^2C_0(q_1,q_2;m,m,m) + \frac{1}{2}\right]\mathrm{Tr}[\gamma^\mu\gamma^\nu\not q_1\not q_2\gamma_5]\,, \quad \text{(F.9)}$$

showing the contribution of the pseudoscalar current proportional to m^2 and the anomalous term. Summation over one complete quark doublet ($\tau_f = \pm 1/2$) cancels the anomaly term and solely the piece proportional to the top-quark mass remains.

JHEP01(2017)020

The function f can be reduced to scalar integrals,

$$f(m;q_1^2,q_2^2,q_3^2) = -\left[3q_1^2q_2^2q_3^2\frac{\delta_2}{\Delta_3^2} - \frac{(q_1^2q_3^2 - m^2\delta_2)}{\Delta_3}\right]C_0(q_1,q_2,m,m,m) + \left[3q_1^2q_3^2\frac{\delta_3}{\Delta_3^2} - \frac{q_1^2}{2\Delta_3}\right]\Big(B_0(q_2,m,m) - B_0(q_1,m,m)\Big) + \left[(3q_1^2q_3^2\frac{\delta_1}{\Delta_3^2} - \frac{q_3^2}{2\Delta_3}\right]\Big(B_0(q_2,m,m) - B_0(q_3,m,m)\Big) - \frac{1}{2}\frac{\delta_2}{\Delta_3} \quad \text{(F.10)}$$

in terms of the kinematic quantities,

$$\delta_1 = q_1^2 - q_2^2 - q_3^2\,, \qquad \delta_2 = q_2^2 - q_1^2 - q_3^2\,, \qquad \delta_3 = q_3^2 - q_1^2 - q_2^2\,,$$
$$\Delta_3 = q_1^2\delta_1 + q_2^2\delta_2 + q_3^2\delta_3\,. \quad \text{(F.11)}$$

In the limit $q_1^2 = 0$ we get

$$\delta_1 = -q_2^2 - q_3^2, \quad \delta_2 = -\delta_3 = q_2^2 - q_3^2, \quad \Delta_3 = (q_2^2 - q_3^2)^2\,, \quad \text{(F.12)}$$

and the result is,

$$f(m;0,q_2^2,q_3^2) = \frac{1}{2(q_3^2 - q_2^2)}\left[1 + 2m^2C_0(q_2,q_3;m,m,m) + \frac{q_3^2}{(q_3^2 - q_2^2)}\Big(B_0(q_3;m,m) - B_0(q_2;m,m)\Big)\right], \quad \text{(F.13)}$$

$$f(0;0,q_2^2,q_3^2) = \frac{1}{2(q_3^2 - q_2^2)}\left[1 + \frac{q_2^2}{(q_3^2 - q_2^2)}\log\left(\frac{q_2^2}{q_3^2}\right)\right]. \quad \text{(F.14)}$$

When we are interested in the special case of an on-shell Z, with $q_2^2 = \varepsilon_2 \cdot q_2 = 0$, $\varepsilon_3 \cdot q_3 = 0$, then we only get a contribution from G_1. The result for G_1 in this limit is $G_1 = f(m;0,q_1^2,q_3^2)$.

References

[1] ATLAS collaboration, *Measurement of the production cross section of jets in association with a Z boson in pp collisions at $\sqrt{s} = 7$ TeV with the ATLAS detector*, *JHEP* **07** (2013) 032 [arXiv:1304.7098] [INSPIRE].

[2] CMS collaboration, *Measurements of jet multiplicity and differential production cross sections of Z+ jets events in proton-proton collisions at $\sqrt{s} = 7$ TeV*, *Phys. Rev.* **D 91** (2015) 052008 [arXiv:1408.3104] [INSPIRE].

[3] W.T. Giele, E.W.N. Glover and D.A. Kosower, *Higher order corrections to jet cross-sections in hadron colliders*, *Nucl. Phys.* **B 403** (1993) 633 [hep-ph/9302225] [INSPIRE].

JHEP01(2017)020

[4] J.M. Campbell and R.K. Ellis, *Next-to-leading order corrections to $W + 2$ jet and $Z + 2$ jet production at hadron colliders*, *Phys. Rev.* **D 65** (2002) 113007 [hep-ph/0202176] [INSPIRE].

[5] J.M. Campbell, R.K. Ellis and D.L. Rainwater, *Next-to-leading order QCD predictions for $W + 2$ jet and $Z + 2$ jet production at the CERN LHC*, *Phys. Rev.* **D 68** (2003) 094021 [hep-ph/0308195] [INSPIRE].

[6] C.F. Berger et al., *Next-to-leading order QCD predictions for Z, $\gamma^* + 3$-jet distributions at the Tevatron*, *Phys. Rev.* **D 82** (2010) 074002 [arXiv:1004.1659] [INSPIRE].

[7] H. Ita, Z. Bern, L.J. Dixon, F. Febres Cordero, D.A. Kosower and D. Maître, *Precise predictions for $Z + 4$ jets at hadron colliders*, *Phys. Rev.* **D 85** (2012) 031501 [arXiv:1108.2229] [INSPIRE].

[8] A. Gehrmann-De Ridder, T. Gehrmann, E.W.N. Glover, A. Huss and T.A. Morgan, *Precise QCD predictions for the production of a Z boson in association with a hadronic jet*, *Phys. Rev. Lett.* **117** (2016) 022001 [arXiv:1507.02850] [INSPIRE].

[9] R. Boughezal et al., *Z-boson production in association with a jet at next-to-next-to-leading order in perturbative QCD*, *Phys. Rev. Lett.* **116** (2016) 152001 [arXiv:1512.01291] [INSPIRE].

[10] A. Gehrmann-De Ridder, T. Gehrmann, E.W.N. Glover, A. Huss and T.A. Morgan, *The NNLO QCD corrections to Z boson production at large transverse momentum*, *JHEP* **07** (2016) 133 [arXiv:1605.04295] [INSPIRE].

[11] R. Boughezal, X. Liu and F. Petriello, *A comparison of NNLO QCD predictions with 7 TeV ATLAS and CMS data for V+jet processes*, *Phys. Lett.* **B 760** (2016) 6 [arXiv:1602.05612] [INSPIRE].

[12] J.H. Kuhn, A. Kulesza, S. Pozzorini and M. Schulze, *One-loop weak corrections to hadronic production of Z bosons at large transverse momenta*, *Nucl. Phys.* **B 727** (2005) 368 [hep-ph/0507178] [INSPIRE].

[13] A. Denner, S. Dittmaier, T. Kasprzik and A. Muck, *Electroweak corrections to dilepton + jet production at hadron colliders*, *JHEP* **06** (2011) 069 [arXiv:1103.0914] [INSPIRE].

[14] S. Kallweit, J.M. Lindert, P. Maierhofer, S. Pozzorini and M. Schönherr, *NLO QCD+EW predictions for V+jets including off-shell vector-boson decays and multijet merging*, *JHEP* **04** (2016) 021 [arXiv:1511.08692] [INSPIRE].

[15] Z. Bern, L.J. Dixon and D.A. Kosower, *One loop amplitudes for e^+e^- to four partons*, *Nucl. Phys.* **B 513** (1998) 3 [hep-ph/9708239] [INSPIRE].

[16] V. Hirschi, R. Frederix, S. Frixione, M.V. Garzelli, F. Maltoni and R. Pittau, *Automation of one-loop QCD corrections*, *JHEP* **05** (2011) 044 [arXiv:1103.0621] [INSPIRE].

[17] J. Alwall et al., *The automated computation of tree-level and next-to-leading order differential cross sections and their matching to parton shower simulations*, *JHEP* **07** (2014) 079 [arXiv:1405.0301] [INSPIRE].

[18] G. Cullen et al., *Automated one-loop calculations with GoSam*, *Eur. Phys. J.* **C 72** (2012) 1889 [arXiv:1111.2034] [INSPIRE].

[19] G. Cullen et al., *GoSam-2.0: a tool for automated one-loop calculations within the Standard Model and beyond*, *Eur. Phys. J.* **C 74** (2014) 3001 [arXiv:1404.7096] [INSPIRE].

JHEP01(2017)020

[20] F. Cascioli, P. Maierhofer and S. Pozzorini, *Scattering amplitudes with open loops*, *Phys. Rev. Lett.* **108** (2012) 111601 [arXiv:1111.5206] [INSPIRE].

[21] C. Frye, A.J. Larkoski, M.D. Schwartz and K. Yan, *Factorization for groomed jet substructure beyond the next-to-leading logarithm*, *JHEP* **07** (2016) 064 [arXiv:1603.09338] [INSPIRE].

[22] S. Dulat et al., *New parton distribution functions from a global analysis of quantum chromodynamics*, *Phys. Rev.* **D 93** (2016) 033006 [arXiv:1506.07443] [INSPIRE].

[23] R. Britto, F. Cachazo and B. Feng, *Generalized unitarity and one-loop amplitudes in $N = 4$ super-Yang-Mills*, *Nucl. Phys.* **B 725** (2005) 275 [hep-th/0412103] [INSPIRE].

[24] R. Britto, B. Feng and P. Mastrolia, *The cut-constructible part of QCD amplitudes*, *Phys. Rev.* **D 73** (2006) 105004 [hep-ph/0602178] [INSPIRE].

[25] S.D. Badger, *Direct extraction of one loop rational terms*, *JHEP* **01** (2009) 049 [arXiv:0806.4600] [INSPIRE].

[26] J.M. Campbell and R.K. Ellis, *An update on vector boson pair production at hadron colliders*, *Phys. Rev.* **D 60** (1999) 113006 [hep-ph/9905386] [INSPIRE].

[27] J.M. Campbell, R.K. Ellis and C. Williams, *Vector boson pair production at the LHC*, *JHEP* **07** (2011) 018 [arXiv:1105.0020] [INSPIRE].

[28] J.M. Campbell, R.K. Ellis and W.T. Giele, *A multi-threaded version of MCFM*, *Eur. Phys. J.* **C 75** (2015) 246 [arXiv:1503.06182] [INSPIRE].

[29] G.J. van Oldenborgh and J.A.M. Vermaseren, *New algorithms for one loop integrals*, *Z. Phys.* **C 46** (1990) 425 [INSPIRE].

[30] G.J. van Oldenborgh, *FF: a package to evaluate one loop Feynman diagrams*, *Comput. Phys. Commun.* **66** (1991) 1 [INSPIRE].

[31] R.K. Ellis and G. Zanderighi, *Scalar one-loop integrals for QCD*, *JHEP* **02** (2008) 002 [arXiv:0712.1851] [INSPIRE].

[32] S. Carrazza, R.K. Ellis and G. Zanderighi, *QCDLoop: a comprehensive framework for one-loop scalar integrals*, *Comput. Phys. Commun.* **209** (2016) 134 [arXiv:1605.03181] [INSPIRE].

[33] L.J. Dixon, *Calculating scattering amplitudes efficiently*, in *QCD and beyond. Proceedings, Theoretical Advanced Study Institute in Elementary Particle Physics*, TASI-95, Boulder U.S.A. June 4–30 1995 [hep-ph/9601359] [INSPIRE].

[34] R.K. Ellis, Z. Kunszt, K. Melnikov and G. Zanderighi, *One-loop calculations in quantum field theory: from Feynman diagrams to unitarity cuts*, *Phys. Rept.* **518** (2012) 141 [arXiv:1105.4319] [INSPIRE].

[35] R.K. Ellis, W.J. Stirling and B. Webber, *QCD and collider physics*, *Camb. Monogr. Part. Phys. Nucl. Phys. Cosmol.* **8** (1996) 1 [INSPIRE].

[36] Z. Bern, L.J. Dixon, D.A. Kosower and S. Weinzierl, *One loop amplitudes for $e^+e^- \to \bar{q}q\bar{Q}Q$*, *Nucl. Phys.* **B 489** (1997) 3 [hep-ph/9610370] [INSPIRE].

[37] J.M. Campbell, R.K. Ellis and C. Williams, *Bounding the Higgs width at the LHC using full analytic results for $gg \to e^-e^+\mu^-\mu^+$*, *JHEP* **04** (2014) 060 [arXiv:1311.3589] [INSPIRE].

JHEP01(2017)020